EXAMINING THE SOURCE OF NITRATE DEPOSITION IN MOJAVE DESERT

by

Christian Chimezie Obijianya

A Thesis

Submitted to the Faculty of Purdue University

In Partial Fulfillment of the Requirements for the degree of

Master of Science

Earth, Atmospheric and Planetary Science

West Lafayette, Indiana

August 2024

THE PURDUE UNIVERSITY GRADUATE SCHOOL
STATEMENT OF COMMITTEE APPROVAL

Dr. Greg Michalski, Chair

Earth, Atmospheric and Planetary Science

Dr. Lisa Welp

Earth, Atmospheric and Planetary Science

Dr. Cliff Johnston

Department of Agronomy

Approved by:

Dr. Marcy Towns

This thesis is dedicated to our mother of perpetual help.

ACKNOWLEDGMENTS

I would like to start by thanking the Almighty God for His grace and guidance throughout this program. My warmest thanks go out to my family for their continuous support and encouragement. I am extremely grateful to my adviser, Dr. Greg Michalski, for his encouragement, guidance, and tireless efforts to help me comprehend the biogeochemistry of the thesis and stable isotopes. I also thank my committee members, Dr. Cliff Johnston, and Dr. Lisa Welp, for their vital contributions.

TABLE OF CONTENTS

LIST OF TABLES

LIST OF FIGURES

ABSTRACT

The origins and deposition of nitrate in dust traps in Mojave Desert are examined in this thesis. Two main hypotheses are tested: (1) most of the dust in the traps comes from local soil, implying that the nitrate content is primarily derived from the soil; and (2) wet deposition is the primary source of nitrate found in the environments, implying that precipitation processes play an important role in nitrate accumulation. To test these hypotheses, we collected data from 11 dust trap from locations in of the US Geological Survey's long-term investigation of dust composition and influx rates. Dust and soil samples were analyzed for ions to determine their origins and the contributions of local vs distant sources. Our findings show that the fraction of soil-derived nitrate ($f_{soil}NO_3^-$) is consistently low at all traps, hardly reaching 0.03, whereas the atmospheric nitrate percentage ($f_{atm}NO_3^-$) is usually close to or equal to 1. This shows that atmospheric sources play a substantial role in the nitrate levels detected in dust traps. Nitrate contributions are also significantly influenced by sedimentary and geological settings, such as the distinctions between alluvium and playa regions. Playas, which are composed of silt and clay, may have higher nitrate concentrations than alluvial plains, indicating that external dust inputs are significant. The second hypothesis's results show that nitrate deposition in the study area is primarily from dry sources, with dry deposition values ranging from 0.68 to 10.84 NO_3^-/kg/ha/yr, averaging 4.12 NO_3^-/kg/ha/yr, and wet deposition values averaging 1.09 NO_3^-/kg/ha/yr. This observation challenges the hypothesis that wet deposition is the primary source of nitrate. The dominance of dry deposition is further supported by low amounts of precipitation and a weak correlation between precipitation and dust deposition. This study concludes that although local soil has a role in nitrate levels in dust traps in the study site, it is not the primary source, external sources and dry deposition account for the majority of nitrate in the dustpan

1. INTRODUCTION

1.1 Background

The formation of soil in semi-arid regions is significantly shaped by various forms of sediment deposition, aeolian processes, and internal transformations. This includes distal sediments captured by surface runoff, the accumulation of solid material from the atmosphere, dissolved compounds in precipitation, and the transformation of organic and inorganic matter by physical and biologic processes. In an examination of three alluvial piedmonts in the Sonoran Desert near Tucson, Arizona, McAuliffe (1994) identified intricate patterns of geological landforms. These patterns emerged from the landscape's erosion and the intermittent build-up of alluvial deposits, leading to stark contrasts in soil ages and profiles. Similarly, Nettleton et al., (1975) conducted research on soil and landscape within Nevada's Lake Lahontan drainage basin and adjacent alluvial fans near Phoenix, and the Mojave Desert in California. Their findings revealed diverse soil ages and classifications related to sediment accumulation. While surface sediment transport is important, soils found in arid and semi-arid environments also exhibit pedogenic characteristics caused by the deposition of atmospheric material and the infiltration of water, which can cause leaching of soil ions, including nitrate, while also inducing biologic activity that can both produce and consume nitrate and other water soluble ions (Ducloux et al.1995).

Due to aridity, desert soils can release various sized particles into the atmosphere that can, depending on wind currents, be transported locally or across vast distances, before being deposited. This particle emission from soil is primarily a result of processes that depend on the soil particle size (mass) distribution. The first process is surface creep, where particles ranging from 0.5 mm to 1 mm in diameter simply move along the surface by the wind because they are too large to be lifted into the air but can collide with and dislodge other smaller particles. Saltation refers to soil particles that are propelled by wind in a layer just above the ground's surface. These particles are typically middle-sized soil particles (0.1–0.5 mm in diameter) and the impact of saltating grains can dislodge even smaller soil particles that can be suspended in the air, a process called sandblasting. Finally, suspension occurs when very fine silt and clay particles, and organic matter, (particles < 0.1 mm in diameter) are lifted into the air by wind. All these processes are initiated

when the wind's shear stress overcomes the resistance of surface materials to detachment and subsequent transport Shao et al., (1993) and the entire phenomenon is known as wind erosion. The extent of wind erosion is influenced by factors such as soil moisture, surface roughness, grain size, and organic content of the soil. The particle size distribution generated during these wind events depends on wind speed and recent wetting and drying events. Likewise, the size distribution of the deposited dust will also depend on wind speed but also on distance from the source region. In this context, "dust" refers to the mechanical suspension of surface material, mainly soil particles, into the atmosphere and can transport elemental and ions contained in the soil.

Since the elemental composition of soil particles often differs between particles sizes, the elemental and ion composition of dust may differ from bulk soil composition from which it was derived. Studies have shown that both source soil and transported dust samples maintain consistent refractory elemental ratios, such as Fe/Al, P/Al, and P/Fe that act as a tracer for where the dust originates. In contrast, Guieu et al., (2002) observed that soil samples from dust-generating regions in the Sahara have a wider variety of elemental concentrations than the elemental concentrations found in transported Saharan dust. Huang et al., (2010) noted water-soluble salts were found in dust aerosols, within the source region were altered during transit. Thus, the transport of ions and elements via dust entrainment and deposition may be more complex than the simple translocation of soil particles.

The accumulation of chemical compounds derived from dust deposition can have an impact on ion leaching long after their deposition, altering soil nutrient dynamics. According to Rosenstock et al. (2019), excessive leaching of base cations from soil continued because of previous sulfur accumulation, even though sulfur deposition had significantly decreased. Between 1994 and 2005, this study found that the decrease in soil water calcium (Ca) concentration was more pronounced than the reduction in magnesium (Mg), and this was attributed to a decrease in atmospheric Ca deposition. Changes in the atmospheric inputs of these elements can have an impact on the low exchangeable pools of Ca and Mg in soils impacted by long-term deposition (Rosenstock et al., 2019) . The atmospheric conditions also greatly influenced the formation of salt deposits in desert regions (Álvarez et al., 2016; Pérez-Fodich et al., 2014). Soil slat development processes in desert regions such as the Mojave Desert can be better understood by defining the rates and sources of ions, particularly nitrate, throughout the region.

Any accumulation and preservation of nitrate in soils is heavily influenced by the processes in the nitrogen cycle. One of the main mechanisms influencing biogeochemical cycles on Earth is the chemical conversion of nitrogen (N) compounds in the troposphere (Gruber & Galloway, (2008). Nitrogen makes up 78% of the atmosphere's overall mass, but it is biologically inert. For biological systems to remain functional, special chemical or biological mechanisms have evolved to convert N_2 into more useful forms of N (reactive nitrogen) like nitrates, nitrites, and ammonium by processes called nitrogen fixation (Gruber & Galloway, (2008). In natural ecosystems one of the main processes responsible for new nitrogen inputs is atmospheric deposition, which can be further divided into dry deposition and wet deposition. Dry deposition is the uptake of reactive gases by surfaces, such as nitric acid ($HNO_3(g)$), or gravitational settling of atmospheric material such as dust that may contain N compounds like nitrate and ammonium. Wet deposition is when soluble compounds, such as dissolved nitrate, is deposited to the surface as rain, fog, or snow. Therefore, for N deposition to be effective, N_2 needs to convert into reactive and soluble compounds such as $HNO_3(g)$, dissolved NO_3^- or particulate matter such as nitrate aerosols, by the chemistry of reactive nitrogen.

Reactive nitrogen compounds are a group of key chemical components in the atmosphere, governing atmospheric reactions in both the troposphere and the stratosphere (Crutzen, (1979)) , and acting as links in global biogeochemical cycles (Galloway et al., 2004). They are present in the atmosphere mainly in the form of nitrogen oxides ($NOx = NO + NO_2$) as a consequence of both natural and anthropogenic processes (Logan, (1983)). NOx can be converted to nitrate (NO_3^-) aerosols or nitric acid (HNO_3^-) (Finlayson-Pitts & Pitts, 2000) or other species via homogeneous and heterogeneous reactions in the atmosphere. Gaseous nitrogen and its fixation by atmospheric oxygen are the first step in the nitrogen cycle in the troposphere.

$$O_2 + N_2 \Rightarrow 2NO \qquad \text{R1}$$

The above reaction takes place at very high temperatures and could be aided by the automobile engines combustion or through the energy from lightning. Nitrogen monoxide, or NO, is the primary type of nitrogen oxide that is first introduced into the atmosphere. Subsequently, NO responds quickly in multiple ways. Because of the comparatively high quantity of O_3 the quickest pathway in the troposphere is through its reaction with ozone (R2). Immediately after the

formation of NO_2, it undergoes photolysis (R3) using UV photons (< 430 nm) and regenerates NO (Hall & Blacet, 1952) .

$$NO + O_3 => NO_2 + O_2 \quad R2$$

A null cycle that takes place in less than a minute between NO_2 and NO and gives no yield effect to O_3 always happens in the daytime. Thus, the new reaction between the two species gives rise to a chemical family called NOx. Hence, a fraction of NO_2 formed in R2 above reacts with O_2 in the troposphere to form O_3.

$$NO_2 + h\nu => NO + O \quad R3$$

$$O + O_2 + M => O_3 + M \quad R4$$

where M can be any chemical species in the troposphere.

The loss of NOx signals the end of the catalytic cycle in the daytime by its oxidation to HNO_3 by OH radical.

$$NO_2^- + OH + M => HNO_3^- + M \quad R5$$

Due to the absence of OH radical in the nighttime, a different set of reactions takes place to form HNO_3^- For NO_X to be lost at night, NO_2 is first oxidized by O_3. Into the nitrate radical

$$NO_2 + O_3 => NO_3^- + O_2 \quad R6$$

The formation of NO_3^- which has different values depending on the location can vary from few ppt in remote areas to thousands of ppt in polluted areas because of emission of burnt fossils. NO_3^- in this set of reactions can serve as a nighttime sink for some volatile organic chemicals (VOCs) through the addition as well as H atom abstraction reactions.

$$NO_3^- + RH ==> HNO_3^- + R \quad R7$$

NO_3^- reacts with NO_2^- equilibrating with gaseous dinitrogen pentoxide N_2O_5.

$$NO_3^- + NO_2^- <=> N_2O_5 \quad R8$$

N_2O_5 is an important source of nitric acid in the nighttime reaction because of hydrolysis on wet surfaces and aerosol particles that can be deposited through wet and dry deposition.

Surface

$$N_2O_5(g)+H_2O \text{ ======> } 2HNO_3 \qquad \text{R9}$$

Thus, conversation of nitrogen oxides (NOx) into other reactive nitrogen compounds plays a significant part in the nitrogen cycle, impacting global biogeochemical processes and substantially contributing to the deposition of nitrate to the Earth's surface.

Another important source of nitrate is nitrification is a key process in the nitrogen cycle. Nitrification is the oxidation of ammonia/ammonium to nitrate by microorganisms and regulates ammonium and nitrate levels in soil. Soil nitrification can be influenced by the climate, soil characteristics, and soil microbes. Rainfall is known to affect soil nitrate content (Gu & Riley, (2010)) suggesting that precipitation plays a mediating role in soil nitrification. Generally speaking, nitrification in soil is thought to occur in two stages: ammonia is oxidized to nitrite by ammonia oxidizers, and then nitrite-oxidizing bacteria convert it to nitrate.

According to Martens-Habbena et al., (2009) ammonia-oxidizing bacteria and ammonia-oxidizing archaea are involved in nitrification. Nitrification involves two steps: ammonia oxidizing bacteria like Nitrosomonas reduce NH_4^+ to hydroxylamine, which is then transformed to NO_2^-

$$NH_4^+ + 1.5O_2 \rightarrow NO_2^- + H_2O + 2H^+ \qquad \text{R10}$$

while NO_2^- is converted to NO_3^- by nitrite-oxidizing bacteria like Nitrobacter

$$NO_2^- + 0.5\ O_2 \rightarrow NO_3^- \qquad \text{R11}$$

Nitrate can be lost by denitrification or plant uptake once it has been generated by biological fixation or deposited from the atmosphere to the surface of the desert. The primary method of nitrogen (N) loss in terrestrial ecosystems, known as biological denitrification, is brought about by the continued reduction of NO_3^- to NO_2^-, NO, N_2O, and N_2 (Stevenson, 1982). Due to the low organic matter content, low water content, reduced populations of microbes, aerobic nature, and neutral to basic pH values in desert soils, there is little or no denitrification in the desert regions. Similarly, low plant cover in desert environments reduces plant uptake of NO_3^-. These factors may contribute to the high nitrate concentrations often recorded in arid soils. And since arid soils are a significant source of dust, soil nitrate transport and deposition may occur during dust storms.

1.2 Significance of the study

Global ecosystems are partially shaped by atmospheric deposition, which functions as a dynamic interface between the atmospheric and terrestrial ecosystems. The complex web of interactions arising from the complicated interplay of chemical species transported by the atmosphere has a profound impact on soil formation processes. Soil formation involves a mass balance between inputs and losses integrated across geological timeframes (Amundson, 2004). Input sources such as atmospheric deposition and nitrification may contribute significantly to the nitrate levels in the desert regions. Arid regions have less water availability, which limits nitrate leaching from soils, in contrast to humid climates where chemical weathering and high precipitation cause dissolved ion losses (Amit et al., 1993; Ewing et al., 2006; Quade et al., 1995). In addition, salt and dust deposition from the atmosphere and local substrate sources encourage the net accumulation of nitrate in arid regions (Reynolds et al., 2006). Understanding these different sources is essential for appropriately evaluating the geochemical properties of desert soils. To comprehend the geochemical properties of soils, it is critical to distinguish between these two sources (Vitousek et al., 1999).

The Mojave Desert is a crucial ecosystem in which atmospheric deposition may play an important role in soil formation. This region's dust sources, atmospheric deposition rates, chemical compositions, however, are not fully understood, despite the possible importance of these phenomenon. This gap hinders our capability to properly comprehend the processes of soil pedogenesis in this arid area. Although it is evident that atmospheric deposition is important in the process of the arid soil formation, there are still uncertainties regarding the nitrate composition, and origins of the nitrates found in the arid soils deposited. Our inadequate knowledge of the processes and amounts of atmospheric deposition, as well as the degree of nitrate solubilization from the dust once it reaches the soil, is especially concerning. As a result, determining the nitrate composition, and origins of nitrates that are deposited from the atmosphere is crucial to comprehending the formation of soil in arid regions generally as well as the dominant process governing soil development in desert regions (McFadden et al., 1987; Reheis & Kihl, 1995). Soil development processes in the Mojave Desert will be better understood by describing the sources of nitrate throughout the study site of Mojave Desert.

1.3 Study Site

The driest and most sensitive of the North American deserts is the Mojave Desert (Figure 1). The desert spans over 50,000 square miles, mainly in California, with some areas in Nevada, Utah, and Arizona. It has the Sierra Nevada Mountains to the northwest, the San Miguel and San Bernadino Mountains to the west, the Sonoran Desert to the southeast, the Colorado Plateau to the east, and the Great Basin to the north (Fig. 1.1). The desert is named after the Mojave (or Mohave), an indigenous people who have resided in the desert for thousands of years. This desert is characterized by extreme heat, with precipitation mainly occurring in the fall and winter, limited rainfall in the summer, and the presence of specific plant species (MacMahon & Wagner, 1985) . As indicated by Dwyer et al., (1966) and further affirmed by (USGS, 2000) reveals that annual precipitation ranges from 34 to 310 mm, with the winter season accounting for about 60 to 90% of the total amount. Despite the scarcity of water and the heat of the desert, over 15 million people live in various cities, such as Las Vegas, NV and Barstow, CA in the Mojave Desert. As the climate and land use change, the land becomes drier, and more disrupted, which may increase dust emission (Duniway et al., 2019).

Figure 1.1: The study area; Mojave Desert

1.4 Problem Statement

Research conducted by the United States Geological Survey (USGS), including studies by (Reheis et al., 1995), highlights the significant role of aeolian dust in the development of soils across the Mojave. In a comprehensive five-year study of dust collected from 55 locations in southern Nevada and California, Reheis & Kihl, (1995) revealed regional differences in dust deposition rates, particle sizes, and compositions. These variations are influenced by climate, dust source characteristics, and human activity. Silt and clay deposition rates vary, with the highest average observed in southwestern California at 30 g/m^2/year. The dust flux is affected by mean annual temperature, source characteristics, and precipitation, with alluvial sources contributing more dust than playas. Corroborating these findings, Reheis et al., (2002) noted that modern dust composition is influenced by alluvial sediments, calcareous playas, Owens Lake's anthropogenically affected playa, and emissions. Preliminary findings by Reheis, (1997) indicate that salt-rich dust from Owens Lake playa is deposited over significant distances, extending at least 40 km north and south of the playa.

Mojave soils are rich soluble ions such as calcium, chloride, sulfate, and nitrate (Voigt et al., (2020)) but the contribution from atmospheric deposition is largely unknown. The USGS studies focused on measuring minerals, metals, (Reheis et al., 1995) and slightly soluble compounds like $CaCO_3$ (Reheis et al., 1992) but no quantification of water soluble ions. In arid regions such as the Mojave Desert, where limited rainfall and high temperatures prevail, atmospheric inputs play a crucial role as a primary source of certain ions like nitrate. Consequently, atmospheric deposition may significantly impact soil chemistry and biology. To comprehensively understand soil chemistry and nutrient cycling in deserts like Mojave, it is essential to discern the relative contributions of soil-derived and atmospheric nitrates. This study addresses this knowledge gap by focusing on nitrate levels in Mojave Desert deposition and soils. Given nitrate's role in nutrient cycling, it represents a particularly significant ion. Our investigation aims to verify whether atmospheric sources substantially contribute to the nitrate pool in Mojave soils and visa-versa, whether Mojave soils are contributing significantly to atmospheric nitrate deposition. We achieve this by comparing nitrate levels in vesicular soil with those observed in atmospheric deposition across the region. Consequently, this thesis aims to verify this origin by comparing nitrate levels in the vesicular soil with those in atmospheric deposition within the region. I therefore pose the following scientific questions that will guide our hypothesis:

1.5 Scientific questions

1. What percentage of the nitrate that are caught in the dust trap come straight from the ground?
2. How does the dust trap's nitrate content change in response to precipitation?
3. Can some areas or circumstances be found where the amount of nitrate that accumulates in the trap because of wet deposition is significant?

We proposed two hypotheses to guide our research which are diagramed in Figure 1.2

1. Most of the dust in Mojave dust traps is from soil derived dust, indicating that the nitrate content in dust is primarily derived from the soil itself.
2. In most habitats wet deposition is the primary method of nitrate deposition, suggesting that wet deposition processes are the primary source of the nitrate found in the Mojave dust traps.

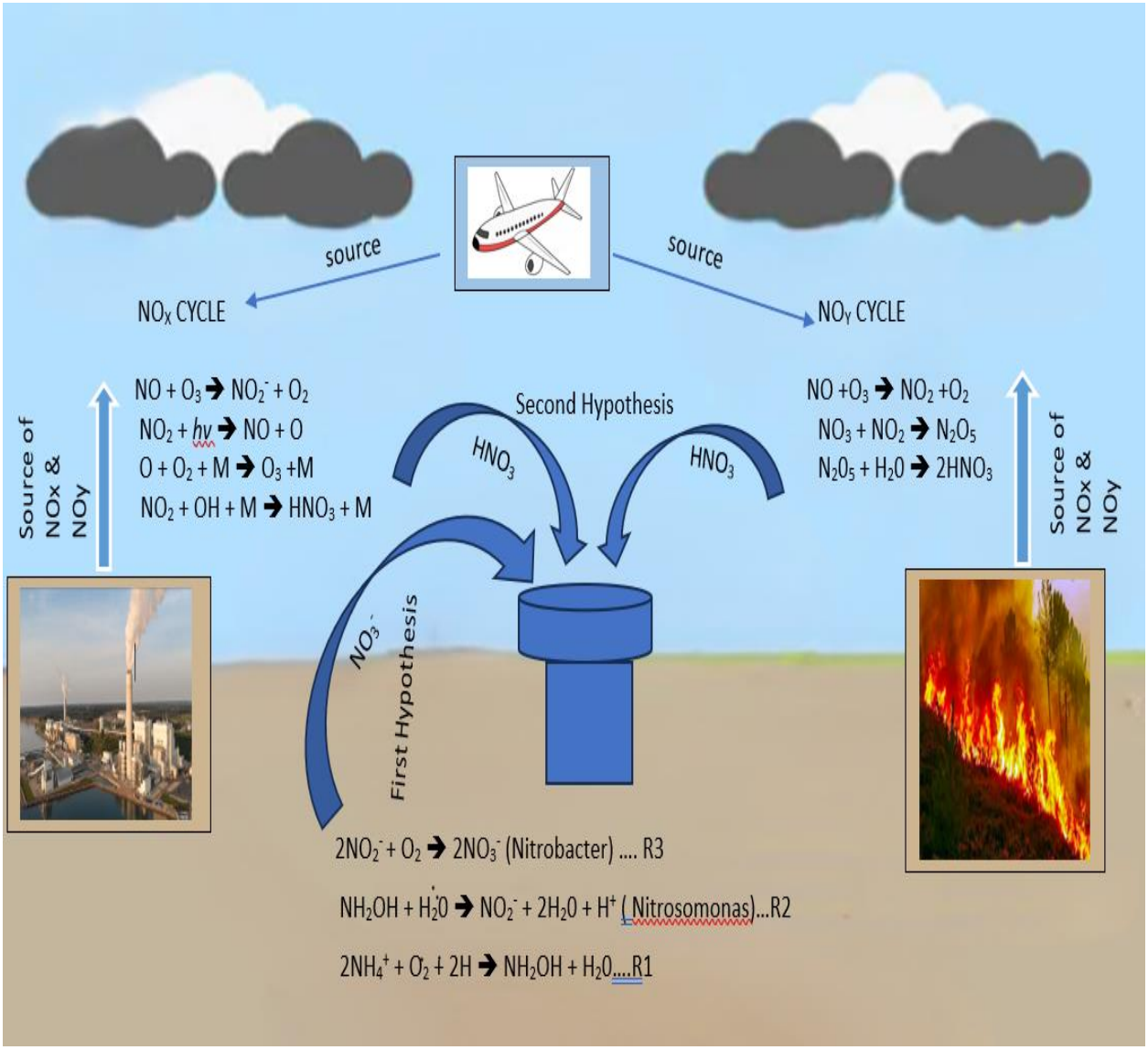

Figure 1.2: NOx and NOy Sources and Atmospheric Cycling. This figure shows the key sources and atmospheric mechanisms involved in the cycling of NOx and NOy. The chemical reactions that transform NOx into NOy species such nitric acid (HNO_3^-) and nitrate (NO_3^-) are shown alongside important sources such as aircraft, biomass burning, and industrial emissions. The diagram also illustrates how different microbial activity (nitrification) and atmospheric processes contribute to the formation of nitrate.

2. NITRATE IN DEPOSITION DERIVED FROM SOIL

First Hypothesis: *The majority of the dust in the dust trap is from the dust in the soil, indicating that the nitrate content is primarily derived from the soil itself.*

2.1 Background for Hypothesis 1

Previous research has provided a number of lines of evidence that much the material mass found in dust collection pans distributed across the Mojave is derived from local and regional soil particles (Reheis & Kihl, 1995). The USGS collected atmospheric materials (dust) samples and sieved them to different particle size fractions and determined that the mineralogical and major-oxide composition of dust trap samples were similar to those of local sand and some silt, while clay and certain silt particles may have traveled from distant sources. Similarly, Reheis et al., (2009) utilized elemental and crustal composition analyses to infer compositional similarities between local soils and modern dust samples in southwestern United States deserts, particularly resembling vesicular (Av) soil horizons. Geochemical analyses of contemporary dust samples have identified four primary sources: (1) alluvial sediments rich in elements such as Hf, K, Rb, Zr, and rare-earth elements, (2) playa deposits characterized by calcareous dust containing Sr associated with Ca, (3) the Owens Lake region, a human-induced playa contributing elements like As, Ba, Li, Pb, Sb, and Sr, and (4) anthropogenic and/or volcanic emissions including As, Cr, Ni, and Sb. Furthermore, Owens Lake and mining operations in the Cerro Gordo district stand out as significant contributors to the composition of dust in Owens Valley, particularly containing elements such as As, Ba, Li, and Pb (Reheis, 1990; Reheis et al., 1995, 2002). A comprehensive analysis spanning from 1991 to 1994, conducted at seven sites within Owens Valley, underscores the dominance of playa surfaces as the principal source of dust in the area (Reheis, 1997). Additionally, a comparative examination between the iron and major-oxide compositions of modern dust and the A and B horizons of Kyle Canyon soils reveals striking similarities, suggesting a plausible local soil origin for pan dust (Reheis et al., 1992). The USGS researchers ultimately concluded that in the Kyle Canyon soils, TiO_2 (titanium dioxide) and ZrO_2 (zirconium dioxide) levels, as well as their ratios, are higher in surface horizons and modern dust than in deeper soils and parent material. In 1999, the measured dust flux ranged from 3.9 to 12.7g/m^2/yr with an average rate of 8.8 g/m^2/yr (Reheis,

2003). In other words, most of the major elements in material found in the dust collectors could be attributed to the wind entrainment and subsequent deposition of local or regional soil particles, or "dust deposition".

In addition to major element analysis, the USGS group (Reheis, 1997) analyzed the trap material for some soluble species in an effort to assess the soil contribution in deposition. In the soils of the Kyle Canyon fans, calcic horizons and calcretes are formed by the dissolution of $CaCO_3$ from eolian dust and calcareous parent material, which is then precipitated as large layers, pedogenic $CaCO_3$ that fills the matrix, and forms clast coatings. The development of opaline or amorphous silica is facilitated by the release of silica ions from the replacement of aluminosilicate grains, which also plays a vital role in the translocation of clays and the oxidation of iron. However, the analysis of soluble species was exclusive to determining the samples' electrical conductivity (EC), which gives an overall measurement of the ions in the dust that are soluble in water, without providing information on the concentrations of specific ions, including nitrate.

Several studies have looked at the distribution of ions in Mojave Desert soils. Marion et al., (2008) observed the highest concentrations of cations (K^+, Ca^{2+}, and Mg^{2+}) in surface soils, while several anions (Cl^-, NO_3^-, and SO_4^{2-}) increased at around a meter deep. These studies indicated that the differences in the nutrient accumulation patterns between cations (K^+, Ca^{2+}, and Mg^{2+}) and anions (NO_3^- and SO_4^{2-}) are most likely due to anions' increased mobility compared to cations. There has been high variability of nitrate concentrations within profiles of Mojave desert soil. Hunter et al., (1982) found the nitrate-N inventory in the upper meter of soil beneath desert pavement is exceptionally high, ranging from 8900 to 12,750 kg ha-1, and is among the highest documented for subsurface (1-30 m depth) inventories (Graham et al., 2008). Deep cores from an uncultivated desert alluvial fan revealed two large volumes of coarse soil with high, unpredictable nitrate levels (20–208 mg L−1 NO_3^--N) at depths of 2.7 to 7.3 meters (Marrett et al., 1990). The origin of these high levels of Mojave nitrates, whether predominately nitrification or atmospheric deposition is still an open question. However, none of the studies conducted in the Mojave area focused on nitrate concentrations in surface soils, which the main layer participating in dust production, which limits the ability to quantify the soil nitrate contributions to atmospheric nitrate deposition.

Nitrate dry deposition refers to the absorption at the earth's surface (soil, water, or vegetation) atmospheric deposition of gas phase HNO_3^- or particulate nitrate. The term "dry

deposition" describes the process of removing particles through diffusion, impaction, interception, or gravitational settling when they collide with hydrological or terrestrial surfaces. According to Driscoll & Martins, (2019), it constitutes 20–30% of all atmospheric deposition, but is difficult to measure and nitrate deposition rates are poorly constrained, and is highly reliant on vegetation features and meteorological conditions. The dry deposition of particles is governed by three primary mechanisms, each dependent on the particle size:

1. Brownian Diffusion: For particles less than 0.1 µm in diameter, the deposition velocity (V.d) is dictated by Brownian diffusion. For particles measuring 0.001 µm, (V.d) may attain values up to 1 cm/s.
2. Gravitational Settling: Particles exceeding 5 µm in diameter exhibit high deposition velocities (V.d)—on the order of several cm/s—primarily due to gravitational forces.
3. Turbulent Processes: Particles within the intermediate size range of 0.1 µm to 5 µm experience the lowest deposition velocities, which are influenced by turbulent processes such as interception and impaction. These processes are comparatively less effective at particle removal.

The relative relevance of each of these physical processes is determined by the particle's proximity to the surface. According to Tegen & Fung, (1994) and Zhao et al., (2014), the distance from the source regions increases the relative importance of dry deposition.

Before being deposited on the ocean or land surface, chemical species and other particles can travel thousands of kilometers after entering the atmosphere (Carlson & Prospero, 1972; Prospero & Carlson, 1972). The displacement of these particulates is subject to a confluence of variables, which include but are not limited to, the dynamics of wind and atmospheric instability, the physicochemical attributes of the dust grains, and the gravitational descent rates. These rates are inherently dependent upon the mass and geometrical form of the individual particles. Once there, they aid in the formation of soils (Glaser et al., 2013; Muhs et al., 2012; Yu et al., 2015) . A lower rate of gravitational settling causes smaller particles to settle at a slower rate and travel longer distances in the atmosphere, but larger-sized particles (>10 µm in diameter) are typically deposited closer to the source (Querol et al., 2019). Research findings have shown that atmospheric depositions are important sources of nutrients in tropical ecosystems (Chadwick et al., 1999; China et al., 2018; Xu-Yang et al., 2022).

This background information can be summarized in the context of my hypothesis 1. First, abundant geochemical evidence shows that most of the solid material collected in the Mojave dust traps is derived from regional desert soils. Secondly, Mojave soils, like other extremely arid environments, are anomalously rich in nitrate relative to temperate soils. Third, entrainment of soil by wind throughout the Mojave can be deposited via dry deposition relatively close to the dust origin. Therefore, there is a logical progression leading to hypothesis 1: That nitrate found in the Mojave dust traps is from the dry deposition of nitrate rich dust derived from Mojave soils.

2.2 Methods for hypothesis 1

The dust-trap sites (Fig 2.2) used in the present study are comprised of a subset of regional sites from Reheis and Kihl, (1995) and sites in Owens Valley (Reheis, 1997). Initially, 46 sampling sites were established across southern Nevada and California, including one site with five dust traps. These sites were supplemented by nine more in 1985, resulting in a total of 55 sites. Annual sampling continued until 1989. Most sites were located at least 0.75 km away from roads or trails to minimize interference, although some dust traps were tampered with and subsequently abandoned (Reheis & Kihl, 1995). Sampling persisted at 37 of these sites with many sites being upgraded to two dust traps in 1989. Additionally, a new site was added every two years until 1999. Currently, a subset of 14 sites is sampled twice a year to monitor seasonal changes in dust deposition and out of this, this thesis only makes use of 11 Trap sites for the study (Table 2.1). The design of the dust traps is described in detail in (Reheis & Kihl, 1995). This study examined the topmost dust-enriched soil layers at eleven sites with dust traps. The surface deposits at most of these sites, which are on alluvial fans or volcanic plateaus of different ages, have a desert pavement with an Av horizon underneath that came from dust. The gravelly desert pavement was taken away, and then soil samples were collected by the USGS between the depth of 0-4 cm deep under the pavement or the ground close to each of the dust traps and a spit was sieved to isolate the sand (<2000 mm) and silt/clay size fractions The anion composition of the dust traps themselves was also previously measured (Michalski, unpublished data)

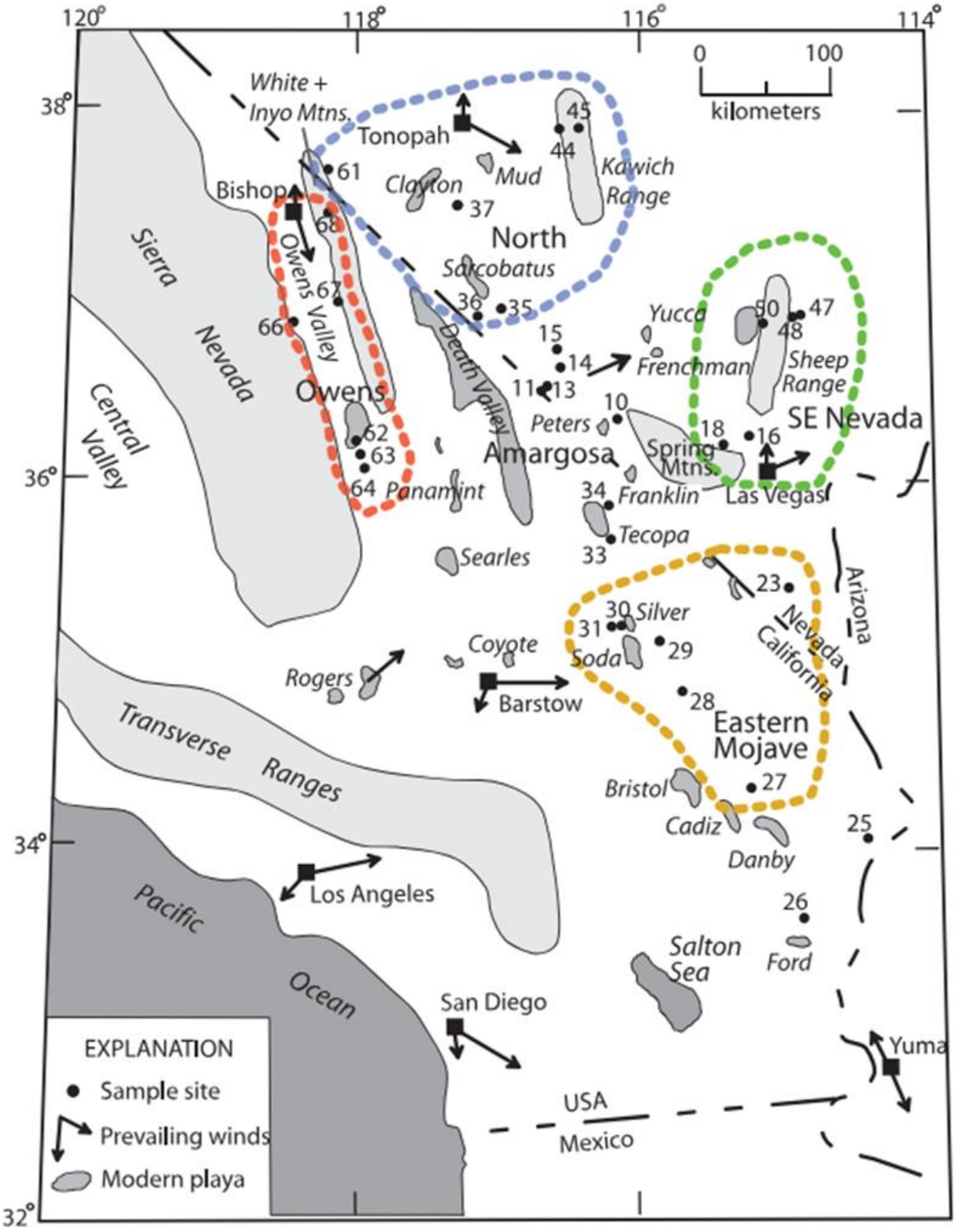

Figure 2.1: Adapted from (Reheis et al., 2009). A map displaying the principal cities, playas, prevailing wind directions, and sample locations. Regional groups of dust trap sites are shown by colored dashed lines: Amargosa and two southern sites (no line), Southeast Nevada (green), Eastern Mojave (gold), North (blue), Owens Valley (red), and Southeast Nevada (green).

2.3 Preparation of soil samples

Water soluble ions were extracted from the soil samples and analyzed using established techniques. The samples were first placed in 15ml vials for initial measurement before being transferred to 30ml vials. 25ml DI water was added to the samples to dissolve the soluble salts. To ensure thorough mixing, the Vetox machine was employed to vigorously blend the soil sample and water for approximately 3-5 minutes until a homogeneous mixture was attained (Fig 2.2). Following mixing, to separate the sediment from the water, the mixed sample was centrifuged for 15 minutes, and the supernatant was decanted and was carefully filtered out using 0.2 micro pore filter paper using a vacuum filter. The anions in the samples were identified based on the retention time and quantified using ion chromatography (IC). Most of my research efforts was dedicated to setting up and learning the new IC system acquired by the EAPS department, interfacing it with a high capacity autosampler and conducting quality control experiments to limit between sample carry over, establish limits of detection, and establish calibration accuracy and precision. A range of calibration standards, from 1 ppm to 100 ppm, were employed to determine the concentration with accuracy. The software calculates the specific anion concentrations by measuring the peak area under the time versus conductivity intensity curve. To minimize measurement uncertainty and validate the accuracy of the measurement, this calibration makes sure that anion peaks are identifiable at low concentrations and avoids column saturation at large concentrations.

Figure 2.2: depicts the sequential steps of the experimental procedures of soil samples. (1) Weighing the soil samples using an analytical balance; (2) Mixing the samples with the help of a vortex mixer to guarantee homogeneity; (3) Centrifuging the samples to separate soil particles from the liquid phase; and (4) Filtering the samples with a vacuum filtration system to eliminate any leftover particulates in the extracted solution.

Full details of the IC methodology and development can be found in Chapter 4 of this Thesis.

Table 2.1: Mojave dust trap site locations and descriptions Adapted from (Reheis et al., 2009). This table details traps and sources, including site IDs, local substrate compositions, geographical coordinates (latitude and longitude), altitudes, and area clusters.

Traps/Source	Site ID	Local Substrate	Lat. (N)	Long. (W)	Altitude	Area cluster
T10 Wet playa	Amargosa Flat	Limestone	36.52	116.11	805	Amargosa/other
T26 Dry playa	McCoy Mountains	Metamorphic + Mixed	33.74	115.93	190	Amargosa/other
T28 Alluvium	Kelso Dunes	Rholite + Granite	34.95	115.61	921	E Mojave
T29 Wet playa	Cima Volcanoes	Basalt	35.26	115.73	1257	E Mojave
T30 Dry Playa	Lower silver lakes	Rholite + Granite	35.32	116.12	290	E Mojave
T33 Wet playa	Tecopa South	Metamorphic + Mixed	35.31	116.14	366	Amargosa/other
T34 Wet playa	Tecopa East	Limestone	35.97	116.23	525	Amargosa/other
T44 Alluvium	Bellehelm	Rholite + Granite	38.15	116.63	1815	North
T63 Playa	Haiwee Reservoir	Metamorphic + Mixed	36.22	117.95	1262	Owen Valley
T27 Alluvium	Cadiz Lakes	Rholite + Granite	34.42	115.29	403	E Mojave
T46 Alluvium	Reveille Valley	Rholite + Granite	38.18	116.42	1760	North

2.4 Test for First Hypothesis

The first hypothesis posits that most of the dust collected in the dust trap originates from soil, thereby suggesting that the nitrate content within the dustpan is primarily derived from the soil. To test this hypothesis, I determined the micrograms of nitrate in the dust collected that could have come from soil using the mass of atmospheric deposition (dust) (Rhesis et al 1995) and the NO_3^- concentrations in adjacent soils and ratio that to the total NO_3^- in the dustpan, giving the fraction of nitrate in the dust originating from soil ($f_{soil}NO_3^-$).

$$f_{soil}NO_3^- = \frac{\mu gNO_3^- \text{ (dust from soil)}}{\mu gNO_3^- \text{ (Trap)}}$$

The total micrograms of nitrate in the dust trap (μgNO_3^- (Trap)) have been previously measured by Michalski (unpublished data). The formula that calculates the micrograms of dust NO_3^- that possible could come from soil is:

$$\mu gNO_3^- \text{ (dust from soil)} = \text{dust (g)}\left(f(\text{sc}).\frac{\mu gNO3-(\text{sc})}{\text{g(sc)}} + f(\text{sand}).\frac{\mu gNO3-(\text{sand})}{\text{g(sand)}}\right) \quad \text{Eqn: 2:2}$$

Dust (g) is the mass of the dust sample in grams in each of the traps and *f*(sc) and *f*(sand) are the mass fraction of silt and clay and sand in the dust sample, respectively. Whereas µg NO_3^- (sc) and μgNO_3^-(sand) is the mass of NO_3^- per gram of the silt and clay and sand in the adjacent soils. I measured the nitrate mass content in parts per million (PPM = μgNO_3^-/ml) in the water-soluble extracts of both silt-clay (sc) and sand components of the soil sample from the different locations using the IC and ml refers to the milliliter of the extraction solution (25 ml). Nitrate soil concentrations were quantified as □gNO_3^-/g of soil through a calculation involving the nitrate extraction concentration (□g/ml), the volume extraction volume in ml, and the soil weight in grams.

$$\mu gNO_3^-/\text{g soil} = \frac{\text{Extraction vol(ml)} \times \mu gNO_3^-/\text{ml}}{\text{Weight of soil}} \quad \text{Eqn: 2.3}$$

The μgNO_3^- of both the silty-clay and sand (in trap from soil) was determined using the hypothesis assumption that all material in the trap (trap mass (g)) was derived from soil (Eq. 2.2) From this data, Eq.2.1 was used for determining soil $f_{soil}NO_3^-$, a value that must fall between zero and 1. If the $f_{soil}NO_3^-$ ~ 1 then the approximately all the traps NO_3^- can be attributed to soils and

the data supports hypothesis 1. If, on the other hand, $f_{soil}NO_3^-$ ~ 0 then almost none of the traps NO_3^- can be attributed to soils and the data refutes hypothesis 1 and shows that some deposition source other than soil (dust) deposition is the source of the NO_3^- in the dust pans.

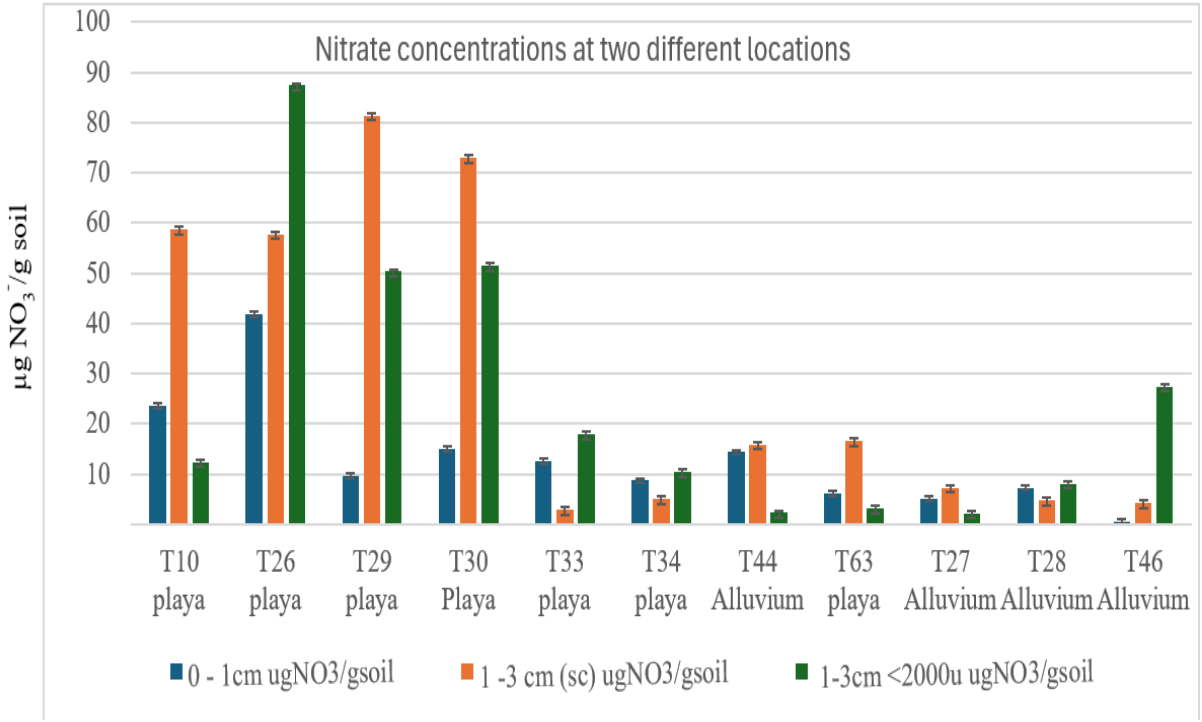

Figure 2.3: Comparison of nitrate levels in soil of various textural class. This table shows the nitrate concentrations in surface soil samples at two different textural class: 1-3 cm (sc) and 1-3 cm <2000u, measured in µgNO_3^-/g soil. at the site. The error bar represents the percentage error.

2.5 Results for Hypothesis 1 test

The results show NO_3^- concentrations in silt/clay and sand are different, that they differed between location, and that all the $f_{soil}NO_3^-$ were ~ 0. Different patterns emerge from the statistical examination of soil nitrate content at different depths. Nitrate concentration (µ gNO_3^-/g soil) at the 0-1 cm layer ranged from 0.6 to 41.8, with an average of 13.2 and a standard deviation of 11.3. Nitrate content varies widely between 1 and 3 cm depth, with a minimum of 2.9, a maximum of 81.4, an average of 26.8±29.6, roughly twice the average NO_3^- concentration of 0-1cm. Nitrate concentrations in the 1–3 cm depth for particles smaller than 2000 microns (sand) range from 2.2 to 87.4, with an average of 23.3 and a standard deviation of 27.6. Nitrate fraction analysis provides further insight into the variations in nitrate, in addition to soil nitrate concentrations. The soil

nitrate fraction ($f_{soil}NO_3^-$) has an average of 0.01, a range of 0.00 to 0.03, and a standard deviation of 0.01. The atmospheric nitrate percentage ($f_{atm}NO_3^-$) is consistently high, with an average of 0.99, a range of 0.97 to 1.00, and a standard deviation of 0.01. These results point to variations in nitrate fractions and distribution, which are crucial for comprehending soil formation and nitrogen cycling in arid ecosystems like Mojave.

2.6 Discussion of results

Table 2.2: This table shows the weight of dust, fractions of sand and soil/silt/clay, and nitrate concentration in dust collected from various traps. Key variables include dust weight (g), fractions of sand (*f*(sand)) and soil/silt/clay (*f*(s/c)), microgram nitrate content per gram of soil/silt/clay (μgNO_3^-/gs/c) and sand (μgNO_3^-/g sand), microgram nitrate from soil (μgNO_3^- dust from soil), microgram nitrate collected in the trap (μgNO_3^- trap), and the fraction of nitrate derived from soil (f_{soil} NO_3^-).

Dust weight	*f* sand	ugNO3/g sand	*f*(sc)	ugNO3 /gs/c	ugNO3 dust from soil	ugNO3 trap	*f* soil NO3	*f* atm NO3
1.30	0.16	12.00	0.73	59.00	58.00	1400.00	0.04	0.96
2.40	0.20	87.00	0.63	58.00	130.00	2500.00	0.05	0.95
4.40	0.11	50.00	0.70	81.00	270.00	2100.00	0.13	0.87
2.10	0.20	51.00	0.69	73.00	130.00	1300.00	0.10	0.90
1.80	0.23	18.00	0.69	3.00	11.00	1000.00	0.01	0.99
2.40	0.16	10.00	0.77	5.00	13.00	3200.00	0.00	1.00
1.10	0.24	2.30	0.70	16.00	13.00	260.00	0.05	0.95
1.30	0.28	3.20	0.65	17.00	16.00	210.00	0.08	0.92
2.40	0.27	2.20	0.63	7.30	12.00	2600.00	0.00	1.00
3.70	0.17	8.10	0.73	4.90	18.00	2800.00	0.01	0.99
0.53	0.27	27.00	0.63	4.20	5.30	1500.00	0.00	1.00

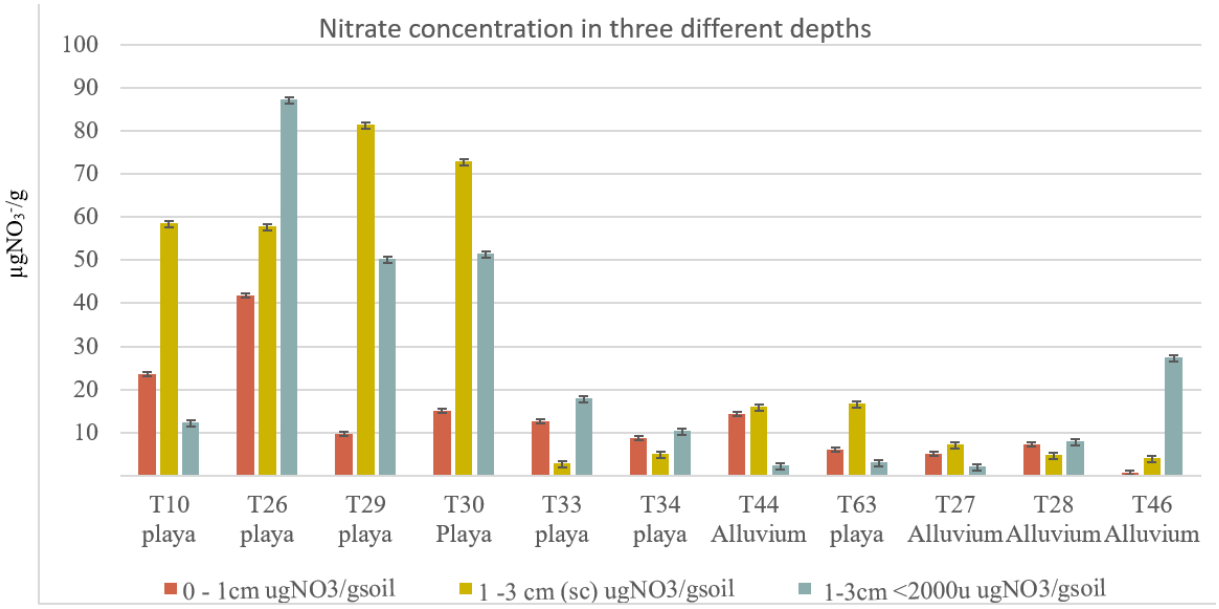

Figure 2.4: The figure compares nitrate (NO_3^-) concentrations in soil samples at three different depths: 0-1 cm, 1-3 cm (sc)silt-clay, and 1-3 cm <2000u (sand), measured in µgNO_3^-/g of soil. Nitrate in Soils Size Fractions. The error bar represents the percentage error.

Due to varying surface features, nitrate leaching in dry desert environments varies greatly (Walvoord et al., 2003) . Surface characteristics can impact the transport and retention of nitrates, therefore regions with low nitrate content, such as the Cadiz lakes (T27), may have less nitrate leaching. However, because this study only looked at nitrate concentrations in the 0-3 cm soil depth, it does not provide enough data to completely estimate the extent of nitrate leaching. Figure (Fig 2.4) illustrates nitrate concentrations at three different depths: 0-1 cm, 1-3 cm (silt-clay), and 1-3 cm (sand) across various locations. It shows that nitrate levels are generally lower at the 0-1 cm depth compared to the deeper layers. For instance, at T29 (playa), the nitrate concentration at 0-1 cm is significantly lower than at 1-3 cm (silt-clay) and 1-3 cm (sand), indicating leaching at the surface. Similarly, T26 and T30 (playa) show higher nitrate concentrations at deeper depths. There are considerable similarities between my findings and those of Graham (2008), who used chloride as a conservative solute tracer to interpret water flux in arid soils. Marrett et al., (1990) similarly reported NO_3^- values ranging from 54 to 208 mg/LNO_3^--N. At depths of 2.6 to 5.7 meters, most of these elevated values were found in samples that were rather shallow. Remarkably, NO_3^- concentrations also became apparent at depth, with thicker layers appearing between 8 and 12 meters down. In addition, Walvoord et al., (2003) presented an intriguing mechanism related to

NO_3^- dynamics. According to their hypothesis, NO_3^- leaches from the soil pool into the subsurface reservoir, which extends just beyond the reach of plant roots. Different soil size fractions have varying nitrate concentrations, suggesting that soil depth and composition may have a major impact on nitrate distribution, with leaching being relevant in the near-surface regions.

2.6.1 Nitrate Distribution in Soil (0-1 cm Depth) Across Size Fractions

The variability in nitrate concentrations across different soil size fractions underscores the influence of soil composition and depth on nitrate distribution. Figure 2.4 illustrates the impact of leaching on soil nitrate levels at various depths. In the 0-0.5 cm soil layer, nitrate concentrations are notably lower, possibly due to leaching of highly soluble nitrate. Conversely, depths of 1-3 cm show higher nitrate levels, suggesting evapo-concentration of nitrates as they leach downwards through the soil. Specifically, the 1-3 cm (sc) fraction ranged from 81.4 µgNO3-/g to 7.3 µgNO3-/g, compared to 9.7 µgNO3-/g and 5 µgNO3-/g at 0.1 cm depth across sampling points T27 to T29. The distribution shows that 1-3 cm (sc) contributed 53.45% and 1-3 cm sand contributed 46.55% to the total µgNO_3^- content of the soil, with a p-value >0.05 indicating no significant difference, likely due to similar soil depths sampled. T29 (Cima Volcanics), which features desert pavement, a surface where at least 65% of the soil is covered by clasts (Anderson et al., 2002; Wood et al., 2002) showed higher nitrate levels than T27 (Cadiz Lakes). The differences may be attributed to variations in geological characteristics and sedimentary deposits (D'Odorico et al., 2007) .

2.6.2 Soil Nitrate as a Function of Location:

The data suggests that alluvium and playa significantly influence nitrate contributions within these catchments. As depicted in Figure 2.4, both Trap 26 and Trap 29, which demonstrate the highest contributions, and Trap 27 and Trap 46, which contribute the least, share some features in common. This is connected to the amount of dust released by these soils due to the composition of their soil particles. The term "playa" refers to the flat bottom of an enclosed basin, which intermittently transforms into a shallow lake (Blank et al., 1999) and (Shaw & Thomas, 1989). Contemporary observations reveal that lakes in arid and semi-arid regions are increasingly impacted by climatic changes and anthropogenic activities, leading to the desiccation of aquatic environments and the exposure of lakebeds (Tao et al., 2015). Gill (1996), Middleton & Goudie

(2006), Prospero et al., (2002), Washington et al., (2006) identifies these desiccated lakes as significant sources of atmospheric dust emissions. Playa surfaces, with slopes less than 0.2 meters per kilometer and composed predominantly of silty clays Rosen (1994) notes, are highly susceptible to aeolian erosion. This susceptibility is evidenced by elevated nitrate concentrations in trap sites on playas compared to those on alluvial plains. Alluvial plains, formed through sedimentation within floodplain soils, consist of gravel, sand, and minor quantities of silt and clay deposited by fluvial processes (Leah et al., 2018) .

Figure 2.4 shows that 80% of traps in the playa areas have higher nitrate levels than those in the alluvium, which might be due to playa mainly consisting of silt and clay or due to intense nitrification that occurs in playa but not is found in alluvium. It has been estimated that anthropogenic playa sources contribute 85% of global anthropogenic dust emissions (Zucca et al., 2021). However, discrepancies arise when comparing nitrate from atmospheric depositions in the dustpans at the study sites. Some alluvium sites (e.g., T44) show high nitrate concentrations at certain soil depths, potentially due to atmospheric deposition from nearby playas or proximity to cities with high anthropogenic emissions of nitrogen oxides (NOx). The higher nitrate concentrations observed in playa traps (e.g., T26, T29, T30) compared to alluvium traps (e.g., T44, T27) support the idea that dust from fine-textured soils (silt and clay) in playas contributes significantly to nitrate levels. The eolian origin can be clearly seen in the silt and clay fractions of sandy soils Dan et al., (1969). The influence of eolian dust on the composition of local soil is dependent on multiple factors, such as proximity to dust sources and the current atmospheric conditions that determine the paths of dust storms (Bodenheimer et al., 2019; Chester et al., 1996; Engelstaedter et al., 2006). Wind-driven sand has played a key part in shaping large portions of the soil formation through the process of rock weathering (Greeley & Iversen, 1985), contributing significantly to soil formation over time (Pye, 1987). The textural differences between playas and alluvial plains influence the dust mass and size fractions, with playas having higher proportions of finer particles that contain nitrate that are more easily transported and deposited as dust. This is evident from the data showing higher nitrate concentrations in playa environments, which are primarily composed of silty clays and are highly susceptible to aeolian erosion.

Playas constitute significant nitrate sources in areas where they are widespread (Gill, 1996) . While playas generally produce high nitrates from arid surfaces, exceptions exist (e.g., T33, T34, and partly T10 with low nitrates). These wet playas contain and emit more nitrates and other

elements due to higher water tables (<4m) (Reynolds et al., 2006; 2009) .This data is consistent with instances observed in the United States' Great Basin: Mono Lake and Owens (dry) Lake (Gill, 1996) have shown that human activity in arid and semiarid environments causes desiccation of saline lakes and playas, resulting in wind erosion and significant aeolian processes. Grass Valley playa in Nevada Young & Evans, (1986) noted substantial subaerial fine particle deposition during winter, and Summer Lake in Oregon (Langbein, 1961) highlighted considerable water level fluctuations in closed lakes in dry and semiarid regions, making them vulnerable to dust production and wind erosion.

2.6.3 Fraction of f_{soil} as a function of location:

The results (Table 2.2) suggest that the nitrate content in the dust trap is not predominantly from soil sources, which contradicts the hypothesis that the bulk of the dust in the dust trap is obtained from the soil. The fraction of soil-derived nitrate ($f_{soil}NO_3^-$) is consistently low throughout all samples, never exceeding 0.03, or 3%, implying that at best only a small proportion of the nitrate in the dust traps comes from the soil. The atmospheric nitrate percentage ($f_{atm}NO_3^-$), on the other hand, is typically close to or equal to 1. This trend demonstrates that atmospheric sources contribute significantly to the nitrate levels measured in dust traps. The idea that external, non-soil sources have a considerable impact on the nitrate content is further supported by the fact that samples with large dust weights and significant nitrate concentrations in the traps (T34, T28) yet show minimal soil-derived nitrate. The results of this study contradict our first hypothesis by showing that most of the nitrate content in the dust traps does not originate from soil sources. In contrast to the atmospheric nitrate fraction, which had an average value of 0.99, the soil-derived nitrate fraction continuously showed low values, never going above 0.03. This significant difference emphasizes how atmospheric sources mostly contribute to the nitrate concentration found in the dust traps. Additionally, the study demonstrated a high degree of variation in nitrate concentrations among various soil size fractions and depths, supporting the idea that atmospheric sources account for most of the measured nitrate levels. These results suggest a shift in focus to investigate wet deposition as a probable major mechanism of nitrogen deposition at the study site.

3. NITRATE WET DEPOSITION IN MOJAVE DESERT

Hypothesis 2. *Wet deposition as the primary method of N deposition in most ecosystems, suggesting that wet deposition processes are the primary source of the nitrate found in the trap.*

3.1 Introduction

Millions of tons of nitrogen dioxide and other nitrogen compounds are annually released into the atmosphere in the United States as a result of both anthropogenic activities like burning fossil fuels and industrial processes, as well as natural processes like soil resuspension and volcanic activity (Galloway et al., 1982; Nriagu & Pacyna, 1988).These nitrogen compounds return to the surface of the Earth through wet and dry atmospheric deposition. Nitrate removal from the atmosphere is mostly accomplished by wet deposition, which includes precipitation such as rain, snow, and fog Zhao et al., (2015). This nitrate deposition in the atmosphere affects soil development.

The term nitrogen “wet deposition" describes the process by which precipitation, such as rain, sleet, or snow, removes reactive nitrogen from the atmosphere (Burns,2003; Clow et al, 2002) (fig. 3.1). According to Yan et al. (2021), this process plays an essential role in regulating the concentration of nitrogen in the atmosphere. There are two main methods of wet deposition. The term "rainout" or "in-cloud scavenging" Hov (1987), describes the scavenging of aerosol particles that are associated with pre-existing cloud droplets or ice crystals inside the cloud, or they can be acting as condensation or freezing nuclei. Washout, also known as below-cloud scavenging, occurs when aerosol particles or soluble gases collide with falling droplets. During wash-out, uptake of gases and/or particles may happen during the downward conveyance of the droplet to the earth's surface in the form of rain, snow, cloud ice, hail, etc.

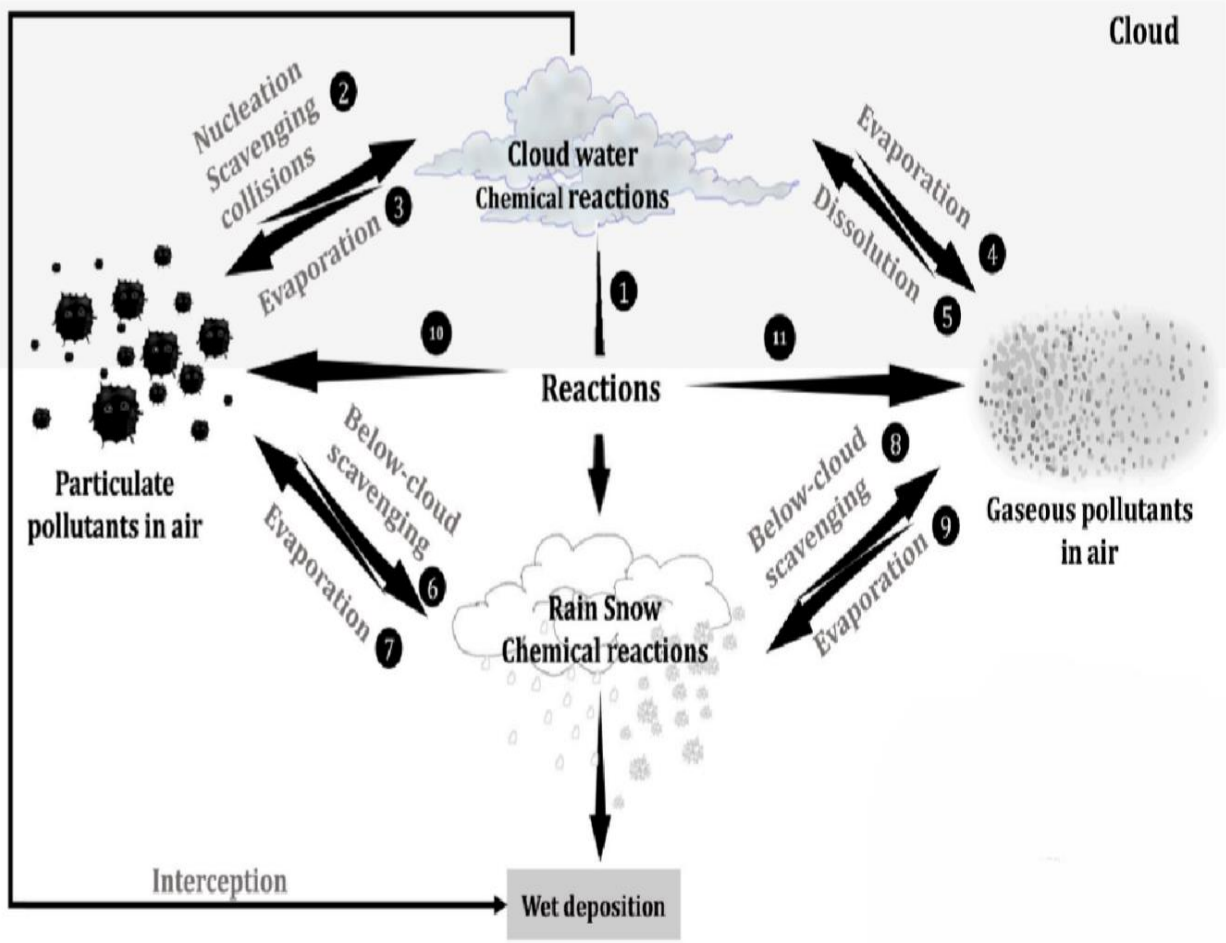

Figure 3.1: shows the Conceptual framework of wet deposition in the study site. Adapted from (Zhang et al., 2021) The main mechanism shown include 1. Cloud water formation,2. Gaseous pollutant in the atmosphere. 3. Particulate pollutant in the atmosphere. 4. Nucleation scavenging collisions. 5. Dissolution and Evaporation .6. Chemical interactions in Cloud Water. 7. Below-Cloud Scavenging. 8. Chemical Reactions in Rain and Snow

3.2 Methods for Hypothesis 2

To measure the deposition of atmospheric components and track the chemistry of precipitation, the US National Atmospheric Deposition Program (NADP) was founded in the late 1970s. The chemical composition of precipitation is greatly impacted by air pollutants, especially NOx, mostly in areas with high precipitation Keresztesi et al.(2020); Guerzoni et al. (1997); Halstead et al.(2000).

The amount of wet deposition is proportional to both the volume of precipitation and the location of the deposition site relative to emission sources. An essential aspect of this process is

the collection and transportation of gases and particulates from the atmosphere by rain, snow, and fog (Tanaka, 2000). Quantification of wet deposition is typically achieved through the deployment of collection apparatus in open fields, designed to capture rain or snow over periods ranging from several days up to one month. To ascertain the fluxes of wet nitrogen (N) (here defined as atmospheric reactive nitrogen (NH_3 and NOy)) deposition, (Zhang et al., 2021) measured the concentrations of Wet N deposition fluxes within the collected precipitation are multiplied by the precipitation volume, employing the following equations:

$$Cw = \sum_{i=1}^{n} (C_i p_i) / \sum_{i=1}^{n} p_i \quad \ldots \qquad \text{Eqn : 3.1}$$

where the concentration of each individual sample, Ci, is weighted by the quantity of rainfall measured for each sample, and Cw is the volume-weighted mean concentration (mg N/L) computed from the n precipitation samples throughout a month or a year.

$$Dw = \frac{PtCw}{100} \qquad \text{Eqn : 3.2}$$

where Pt is the total quantity of all precipitation events (mm), 100 is a unit conversion factor, and Dw is the wet/bulk deposition flux. This is a unit conversion factor that allows the conversion of the total amount of all precipitation events (mm), (Pt) from millimeters to kilograms per hectare (kg/ha). Essentially, it helps standardize the units for comparison.

3.3 Test for Hypothesis 2:

To test this hypothesis, I will compare the dry and wet deposition data to see if they're equal. Dry deposition is calculated as the difference between total (trap) and wet deposition. The nitrate from total atmospheric deposition is calculated using the formula:

$$\text{mmol}NO_3^- m^2/\text{yr} = \frac{\text{mmol}NO3}{(\text{collection time}) \times (\text{pan area}) \times 1000} \qquad \text{Eqn : 3.3}$$

where the collection time ranges from 1.9 to 2.1 years, pan area is 0.05 m^2 and 1000 is the correction factor to convert it to mmol/m^2/yr.

f_{wetDep} = NO_3^-WetDep rate/ NO_3^-TotalDep rate; the fraction of where NO_3^-WetDep rate is the NADP wet deposition rate in mmol $NO_3^-m^2/yr$

If the data shows that wet deposition is comparable to dry deposition, this will imply that wet deposition is the predominant source of nitrate deposition. If differences are found, they could be due to precipitation influencing the concentration. In such a circumstance, I will correlate the total deposition to precipitation data from PRISM to further evaluate this relationship.

3.4 NADP Sites in the Study Area and Years of Operation

The NADP monitoring sites in the research area provide vital information on nitrate deposition patterns across the study area. The Death Valley National Park-Cow Creek site (CA95) operated at an elevation of 125 meters from February 8, 2000, until May 31, 2005. Operating at an elevation of 2066 meters. Red Rock Canyon site (NV00) operated at an elevation of 1137 meters from January 22, 1985, to December 10, 2002. The Bishop site (CA34) operated at an elevation of 1252 meters from March 4, 1980, until June 22, 1982. The Joshua Tree site (CA 67) has an elevation of 1239 and was established on September 19, 2000, and it is still operational.

Table 3.1: shows the Nitrate deposition values (NO_3^-/kg/ha/yr) for wet (NADP) and (dry) dust sources, with corresponding fractions. Dust Traps are chosen and average values of them were taken depending on their proximity to NADP monitoring sites.

Site Name	Trap ID	Traps	Wet Dep. (NO_3^- /kg/ha/yr)	Dry. Dep.(NO_3^- /kg/ha/yr)	Total Depo. NO_3^- /kg/ha/yr)	Std. Dev	Fraction from wet	Fraction from dry
Las Vegas	NV00	50,47,28,18,16	2.39	3.03	5.41	5.97	0.44	0.56
Death Valley	CA95	15,13,10,14,11	0.90	2.08	2.98	4.01	0.30	0.70
Bishop	CA34	68,67,62,63,64	0.83	0.31	1.14	1.80	0.73	0.27
Joshua Tree	CA67	30,31,29,28,27,23	0.26	10.84	11.10	4.99	0.02	0.98

The NO_3^-kg/ha/yr wet deposition from NADP is compared to the site's dust concentration of kg N/ha. However, the kg N/ha value was converted to NO_3^-kg/ha/year using the molecular weight ratio.

$$\text{Conversion factor} = \frac{\text{molecular weight of nitrate}}{\text{molecular weight of nitrogen}}$$

Applying the resultant conversion factor to a given value of Nitrogen will yield an equivalent value in NO_3^- for easy comparison.

Table 3.1 presents the fractions of nitrate deposition from wet (NADP) and dry (dust) sources at various sites. The dust traps used in this study were strategically chosen based on their proximity to NADP monitoring sites. Notably, the amount of nitrate from dry deposition is consistently high across all sites, with values ranging from 0.68 to 10.84 NO_3^-/kg/ha/yr averaging 4.12 NO_3^-/kg/ha/yr. In contrast, the nitrate fractions from wet deposition are lower, averaging 1.09 NO_3^-/kg/ha/yr and ranging from 0.26 to 2.39 NO_3^-/kg/ha/yr. This stark contrast suggests that dry deposition is the predominant source of nitrate deposition at these sites.

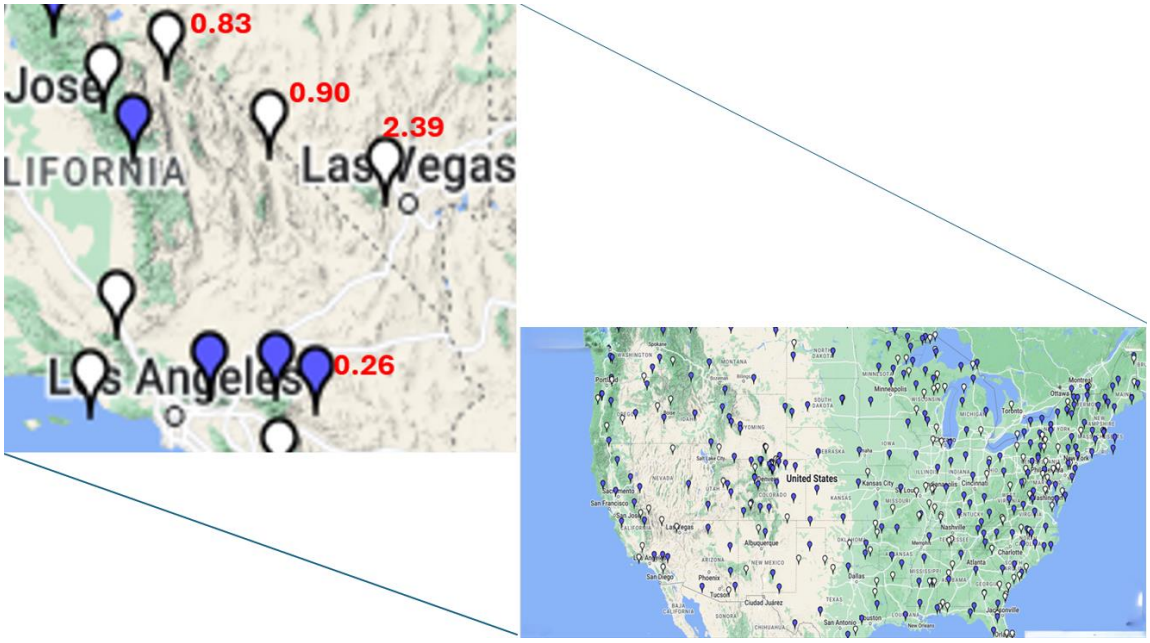

Figure 3.2: Distribution of nitrate wet deposition across United States Adapted from (NADP); This map illustrates the spatial distribution of nitrate wet deposition ($kgNO_3^-$/ha/yr) in the United States. Different deposition rates, ranges from 0.23 to 2.39 kg NO_3^-/ha/yr

These results contradict the hypothesis that wet deposition makes up most of the total nitrate deposition. This study shows that dry deposition is the primary form of NO_3^- deposition in arid environments. This finding is consistent with observations of nitrogen (N) deposition in the western United States made by Fenn et al. (2003) and Li et al. (2016). Their findings demonstrate that nitrogen deposition, which comprises diverse nitrogenous chemicals such as nitrate, varies over the region, ranging from 1 to 4 kg/ha/year to 30 to 90 kg/ha/year. Similarly, Zhang et al. (2021) observed that the western United States has low wet N deposition, ranging from 0.02 to 1.5 kg N/ha/yr. These results, converted to $kgNO_3^-$/ha/yr as explained earlier.

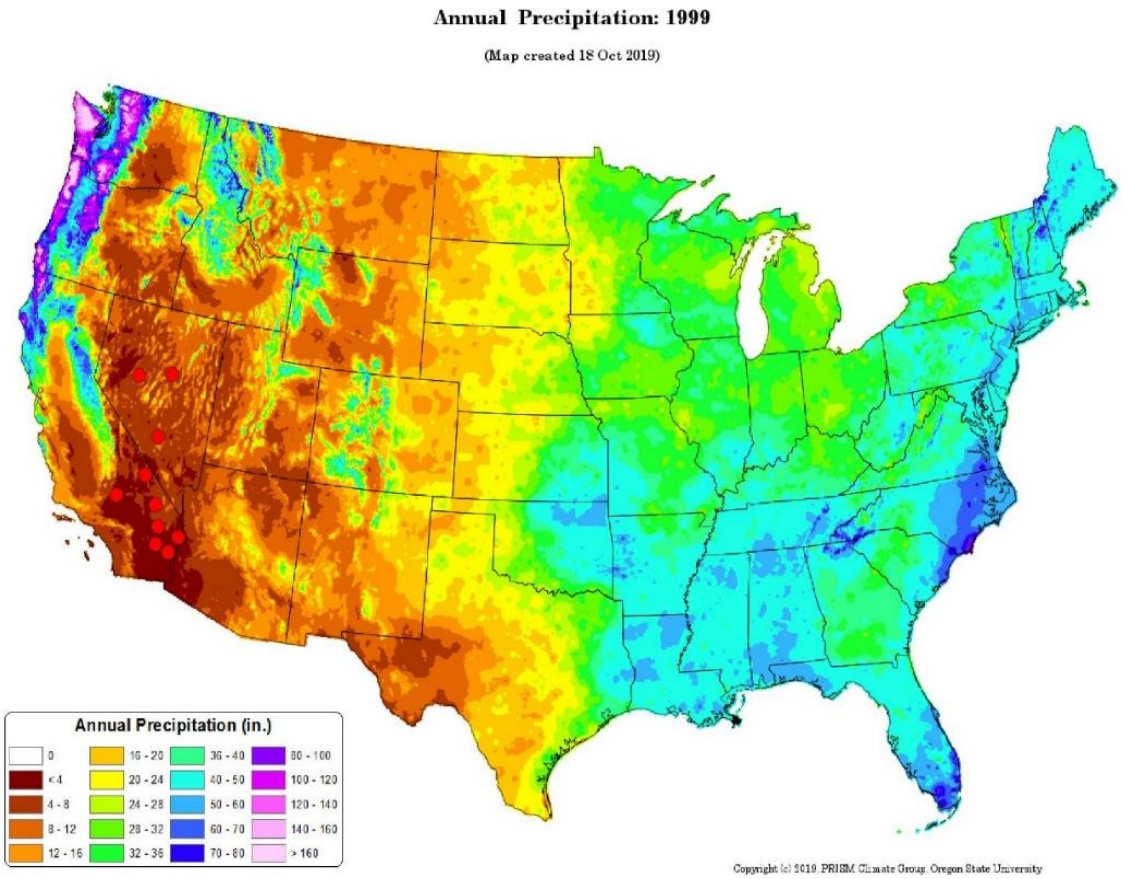

Figure 3.3: The precipitation levels in inches are displayed on this map (PRISM Climate Group, 1999), which shows the yearly precipitation over the United States for the year 1999. The range of colors shows different amounts of precipitation, ranging from dark brown (less than 4 inches) to dark purple (more than 160 inches). The study site locations are indicated by red dots.

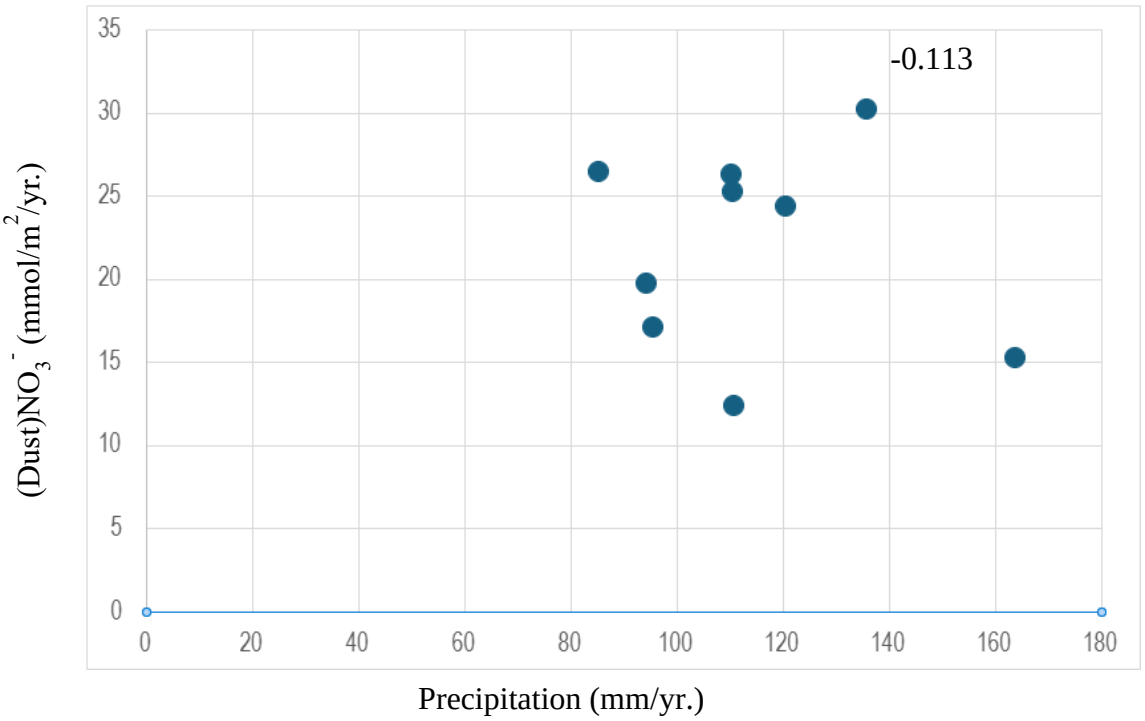

Figure 3.4: Relationship between annual rainfall and total dust deposition in the study site. The scatter plot shows the relationship between annual rainfall(mm/yr) and total dust deposition (mmol/m2/yr).

There was no comparison between wet deposition and dry deposition which gives an insight that precipitation might be the influencing the concentration of the dry deposition, to check if this is true, we used the precipitation dataset from PRISM and with QGIS 3.36, these datasets were integrated into a PRISM map (fig 3.3). An innovative method for precipitation analysis was created at Oregon State University called PRISM (Parameter-elevation Regressions on Independent Slopes Model). It uses point data, digital elevation models (DEM), and geographic information to construct gridded estimates of several climatic parameters, beginning with precipitation and eventually expanding to include temperature, snowfall, and other variables (Daly et al., 1994, 1997). PRISM is a methodically validated technology that uses parameter-elevation regressions on distinct slopes to adapt for and properly represent unique topographic and climatic variables. From the United States to Canada and beyond, this method guarantees strong mapping accuracy in a variety of geographical areas. However, PRISM is subject to limitations, particularly when predicting climate parameters over large elevation ranges using little observational data. These uncertainties are addressed using localized adjustments and validation against accessible

data points, allowing PRISM to efficiently model complicated climatic scenarios (Taylor & Daly, 2004).

The result show that study area is characterized by low precipitation (from less than 0.001In (0.0254mm/yr) to 1.2In (30.48mm/yr)), Research by Al-Momani et al., (2002) and Tuncer et al., (2001) indicate that in arid regions with erratic rainfall, dry deposition predominately constitutes the main source of atmospheric deposition. Our results align with this claim, reflecting a regional average precipitation of approximately 4.4 inches/yr. These results are consistent with the conclusions drawn by Peretti et al., (2020) and Zhang et al., (2018), that fluctuations in precipitation influence the patterns of wet deposition across diverse geographical locations.

Furthermore, the degree and direction of the linear association between the dust deposition and precipitation data was assessed using correlation analysis. This was done by using Pearson correlation coefficient formula below: This analysis hopes to establish whether precipitation and dust deposition are significantly correlated, so shedding light on whether the total deposition was mostly from precipitation.

$$r = \frac{n(\sum xy) - (\sum x)(\sum y)}{\sqrt{[\, n\sum x^2 - (\sum x)^2 \,][\, n\sum y^2 - (\sum y)^2 \,]}}$$

where x is the precipitation data and y are the dust deposition data.

Thus, though the amount of nitrate in the two states used in the correlation may differ as a result, the result is expected to provide valuable insight in the observed relationships. By determining the correlation coefficient's strength and nature, we can make conclusions regarding the predominant form of nitrate deposition in the study areas.

The result (fig 3.4) indicates that there exists a weak negative correlation between the two variables with a p- value of < 0.05. This answers the question that precipitation is most probably not the source of nitrate in the region.

The troposphere's nitrogen oxides (NOx) are known to be generated by industrialization, fuel combustion, and other human activities that release nitrogen into the atmosphere. NOx can easily undergo a number of chemical reactions to produce nitric acid (HNO_3^-). The HNO_3^- can subsequently be integrated into atmospheric particles, which explains why nitrate deposition is elevated in areas near cities such as NV00 near Las Vegas, and Joshua Tree that has several cities close by including Los Angeles that is 173 miles far from it with a population of 642,000 and

13,000,000 respectively in 2020 census exhibits high nitrate deposition. A 50% reduction in overall NOx emissions is expected to result in a 37% decrease in total NO3-deposition, with a combined 74% efficiency in wet and dry deposition (Butler et al., 2005).

This finding is consistent with (Elliott et al., 2007), who measured that the spatial and temporal distribution of nitrate in wet deposition at 33 National Atmospheric Deposition Program - National Trends Network sites in the northeastern and midwestern United States is primarily influenced by nearby stationary source emissions, such as electric generating units. Furthermore, (Barrie & Sirois, 1986) shows that nitrate deposition is higher in urban regions than in rural ones demonstrating the significance of regional variations in nitrogen deposition Sickles & Shadwick, (2007).

The results provided show that industrial and urban emissions have a substantial influence on nitrate deposition, especially in arid regions with minimal precipitation and peculiar atmospheric conditions.

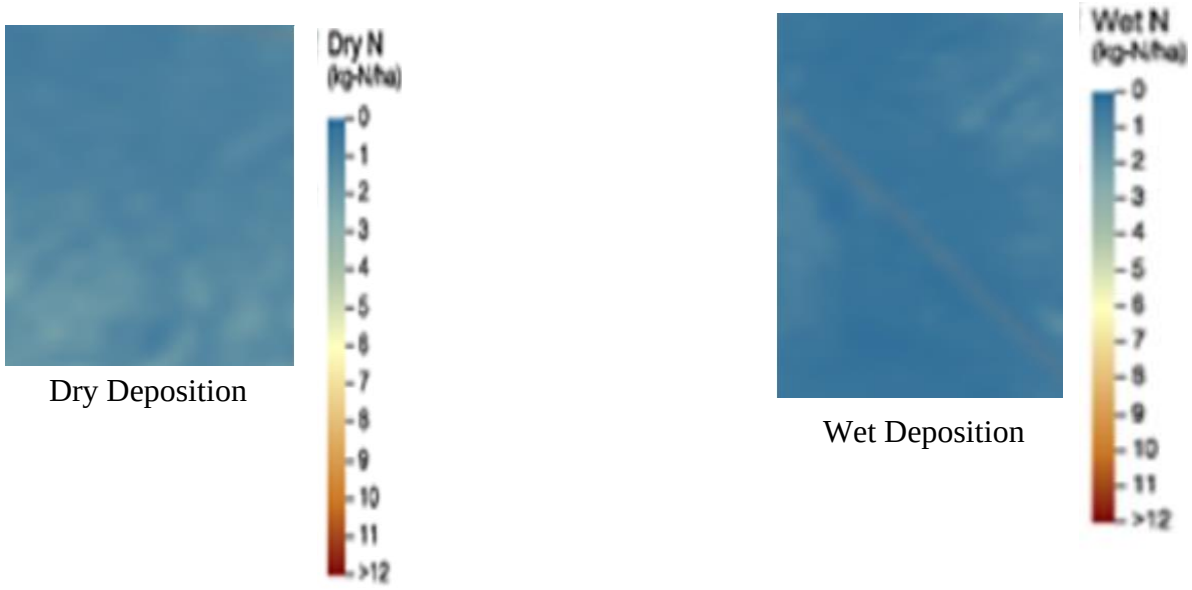

Figure 3.5: Wet and Dry nitrogen deposition across the United States. Data derived from the NADP. The map depicts locations with variable nitrogen deposition levels, measured in kg N/ha, showing places with higher deposition, particularly in the Midwest and parts of California.

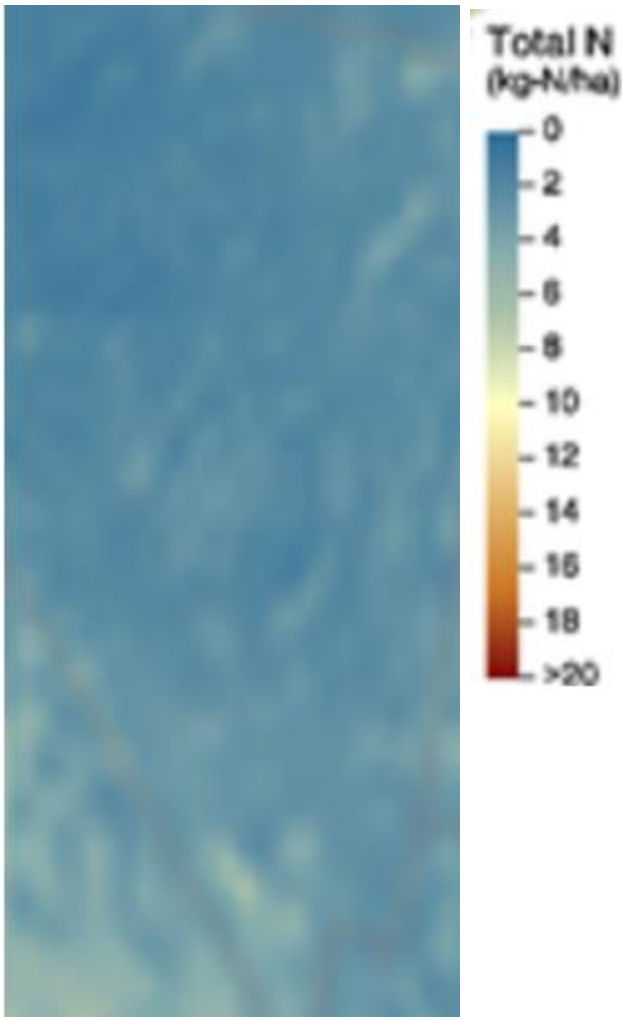

Total Deposition

Figure 3.6: Total nitrogen deposition across the United States. Data derived from the NADP. The map depicts locations with variable nitrogen deposition levels, measured in kg N/ha, showing places with higher deposition, particularly in the Midwest and parts of California.

To further understand nitrate deposition in the study area, I compared my observations with the modeled results from the National Atmospheric Deposition Program (NADP). The analysis utilized data collected from the NADP National Trend Networks (NTN) and unpublished data from Michalski. The dust trap data, which were in proximity to the NTN sites, were averaged to obtain representative values for comparison with the NTN data (Table 3.1). The observational data comprised NADP wet deposition values, atmospheric dust deposition values, and total deposition values (the sum of wet and dry deposition). Additionally, the fractions of total deposition attributed to wet and dry sources were calculated. These observed values were then compared to the modeled

nitrate deposition values provided by NADP to account for areas where monitoring stations were not available. The modeled data from the Community Multiscale Air Quality (CMAQ) model were used to fill in spatial gaps and provide information on chemical species not measured by routine monitoring networks.

When compared to the NADP's modeled values, the results indicated that the modeled observations were approximately 0.5 kg N/ha, 1 kg N/ha, and 2 kg N/ha for wet, dry, and total depositions, respectively. However, converting these values with molecular ratios still resulted in relatively low values. In contrast, the measured nitrate deposition in my study recorded averages of 1.17, 5.88, and 7.05 NO_3/kg/ha for wet, dry, and total depositions, respectively.

Significant differences are shown when comparing the modeled and observed nitrate deposition values. When compared to my observations, the modeled values from NADP underestimate nitrate deposition. These variations highlight the significance of localized precise measurements while evaluating nitrate deposition. The findings imply that, while modeled data might fill in spatial gaps, relying only on models without adequate ground-measurements can result in nitrate deposition underestimations.

4. INSTRUMENTATION

4.1 Introduction to Ion Chromatography

Technical Note: This section of the thesis elaborates on the principles of ion chromatography, its application in analyzing soil samples, and the encountered challenges along with their respective solutions.

4.2 Overview of ion chromatography (IC) and its applications

An instrument called ion chromatography (IC) separates polar molecules or ions in a solution according to the size and charge of each group. After being pumped through an ion-exchange analytical column, the anions in each full soil supernatant sample solution are absorbed onto the column due to ionic interactions with the column resin. This is followed by the elution of the anions from the column and back into solution with a carbonate mobile phase. As the mobile phase moves through the column, the anions elute at different times, varying the conductivity of the solution. Instead of desorbing back into solution all at once, the anions elute at different times.

A conductivity detector is then used to measure the change in conductivity. The retention period is the period between the sample injection into the column and the anion's detection. The unique anions are subsequently identified by correlating each anion retention time with conductivity detection. The biogeochemistry lab's IC equipment was modified to use two analytical columns, one serving as a guard column to separate the sulfate, nitrate, and chloride in each soil solution. The IC equipment was mostly modified to run exclusively in analytical mode.

The analytical mode compares the sample conductivity to standards mixed to known concentrations and uses a determined volume of soil sample solution to pump onto the analytical column to determine the concentrations of each anion.

4.3 Ion Chromatography System components

The ion chromatography system in the Biogeochemistry Lab includes a liquid eluent, high-pressure pump, sample injector, guard and separator column, chemical suppressor, conductivity cell, and data-obtaining desktop. A standard solution is used to calibrate the ion chromatography equipment before running a sample. The data from the sample is compared to the standard to

identify and measure the ions present. A chromatogram (a plot of detector output vs. time) is produced by the data gathering system, typically a computer with chromatography software. Generally, there are six stages of Ion Chromatography analysis:

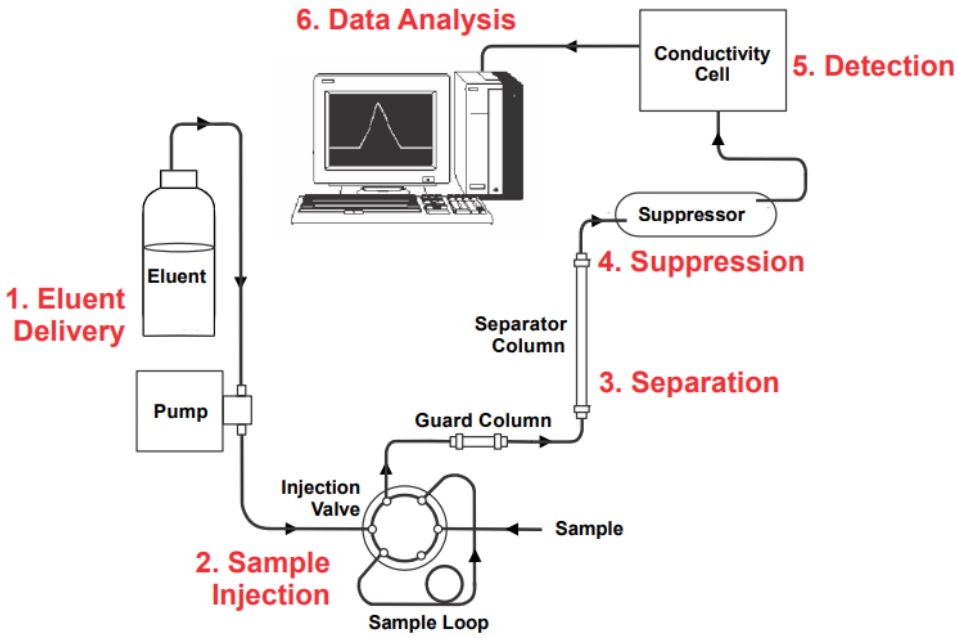

Figure 4.1: (Dionex Aquion Ion chromatography manual, 2016). The figure displays a schematic diagram illustrating the components and structure of an ion chromatography system.

4.3.1 Eluent

The eluent (or mobile phase), a liquid that carries the sample ions through the ion chromatography system. The Dionex Aquion delivery system is isocratic, meaning that the eluent does not change its composition or concentration during the run. The eluent is pushed by a pump through an injection valve that ensures accurate and consistent sample volumes. The eluent choice depends on various factors, such as the sample type and the separation column. Hydroxide or carbonate are the most widely used eluents as the eluting anions. They have different properties that are explained below.

4.3.2 Carbonate Eluent

Carbonate eluent has been the conventional choice for anion analysis. It is a water-based solution of carbonate and hydrogen carbonate salts that allows adjusting the total ionic strength

and the ratio of monovalent (HCO_3^-) to divalent (CO_2^-) ions to achieve the best retention time and selectivity among monovalent and multivalent sample ions. When carbonate eluent flows through the suppressor, it produces carbonic acid ($H_2CO_3^-$). Carbonate eluents typically have an eluate pH of around 4 due to the presence of carbonic acid, resulting in a conductivity of 10-20 $\mu S \cdot cm^{-1}$. At low PH, analytes that have turned into strong acids like nitrate (NO_3^-) will split up completely, thus, the pH of the eluate affects the rate of splitting of weak acids. For instance, only about 20% of acetic acid splits up at this pH, and since only split-up ions cause electrolytic conductivity, a lot of it reaches the detector without giving any signal.

To prepare the eluent, freshly drawn, deionized lab water that has a specific resistance of 18.2 megohm-cm (low conductivity) must be used. Deionized water should not be stored in glass or plastic containers, as this will make the conductivity to quickly increase, and the eluent quality will be reduced. The sodium hydroxide used must be very pure. To achieve the lowest possible back-ground conductivity, the hydroxide eluents must be made from 50 weight percent NaOH or KOH without carbonate.

4.3.3 Eluent Pump

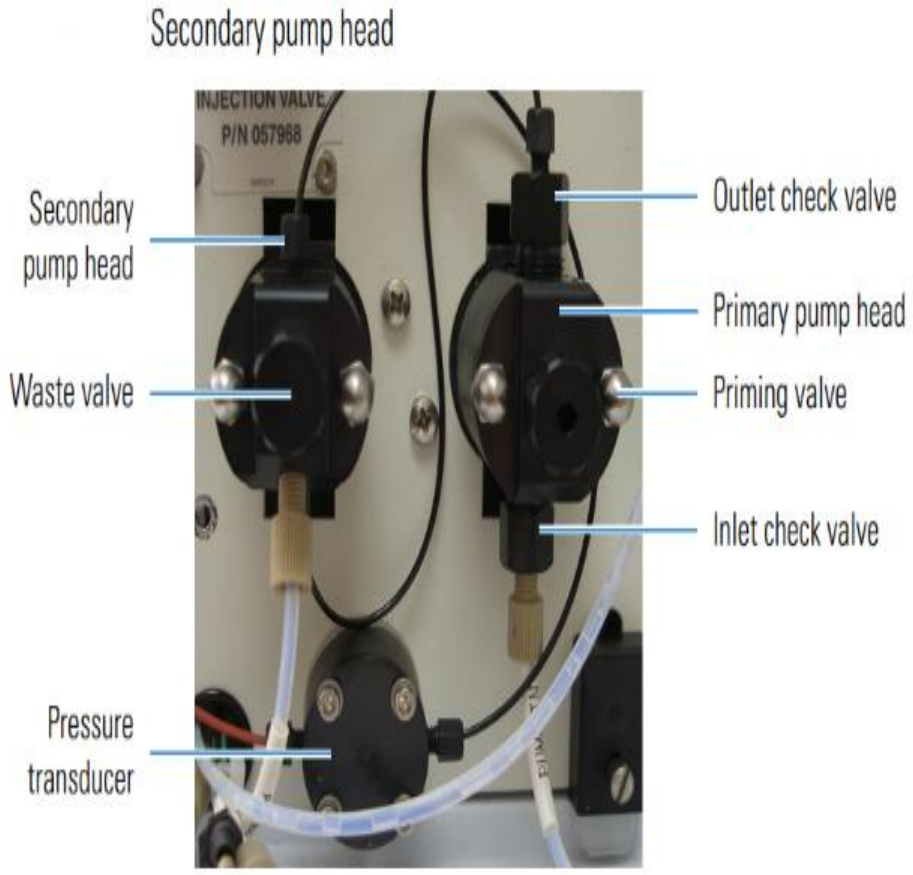

Figure 4.2: shows the secondary head pumps and their parts in an ion chromatography system.

The Dionex Aquion is equipped with a serial double piston pump that simplifies pumping in the eluent. The flow rate can be adjusted to a minimum of 0.00 ml/min or between 0.05 and 5.00 ml/min. However, for optimal performance, it is recommended to set the flow rate between 1.2 (4mm column) and 0.3 ml/min (2mm column). To turn off the pump, set the flow rate to 0.00 ml/min.

4.3.4 Sample Injection

A sample loop is filled with a liquid sample, either manually or via an autosampler. Upon activation, the Dionex Aquion injects the sample into the eluent stream. The eluent and sample are then driven by the pump through the guard and separator columns, which are tubes made of

chemically inert material and filled with a polymeric resin. The guard column functions to remove contaminants that could potentially damage the separator column.

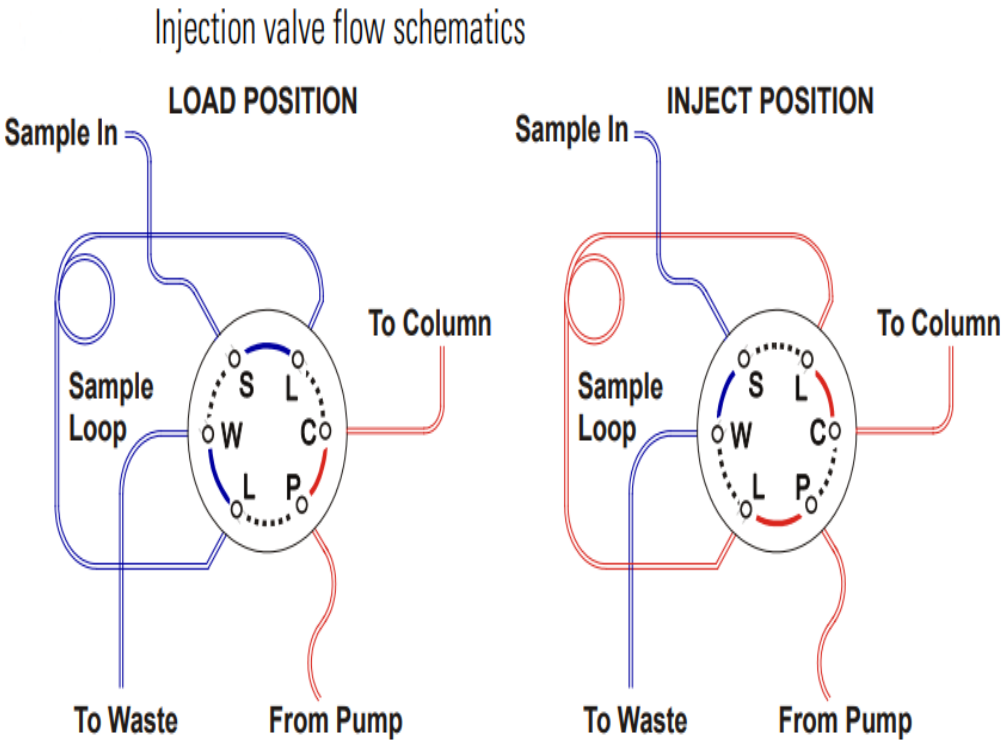

Figure 4.3: Injection Valve Flow Schematics:(Dionex Aquion Ion Chromatography, 2016) The diagram depicts the flow routes of the injection valve in both the load (left) and inject (right) positions, indicating how the sample enters the chromatography system.

During the loading phase, the sample solution enters the sample loop, while the eluent is directed towards the column. The sample loop within the chromatography system is designed to hold the sample in preparation for injection. Meanwhile, the eluent, serving as the solvent, bypasses the sample loop and travels directly from the pump, through the valve, and into the column. Samples proceed from the automated sampler line or syringe, pass through the valve, and fill the sample loop.

When the injector is switched to the inject position, the eluent propels the sample from the loop into the column for analysis. At this stage, the injection valve is filled with the eluent. Following the sample loading and the toggling of the injection valve to the inject position, the eluent flows through the sample loop in the injection valve. Subsequently, the mixture passes through the suppressor, guard, and separator columns.

The mixture then enters the cell via the suppressor, where analytes are detected, and their signals are transmitted in digital form to the Chromeleon software. After exiting the cell, the mixture is rerouted back to the suppressor, which acts as the regenerant chamber's water source. Finally, the flow is directed to waste disposal.

4.3.5 Separations

After exiting the guard column, the sample ions are directed to the analytical or separation column. Sample ions are separated in the separation column as the sample and eluent move through the column. To achieve this separation, the Dionex Aquion makes use of ion exchange chromatography. In this procedure, various sample ions move through the ion chromatography (IC) column at different rates based on how they interact with the ion exchange sites.

4.3.6 How the column work

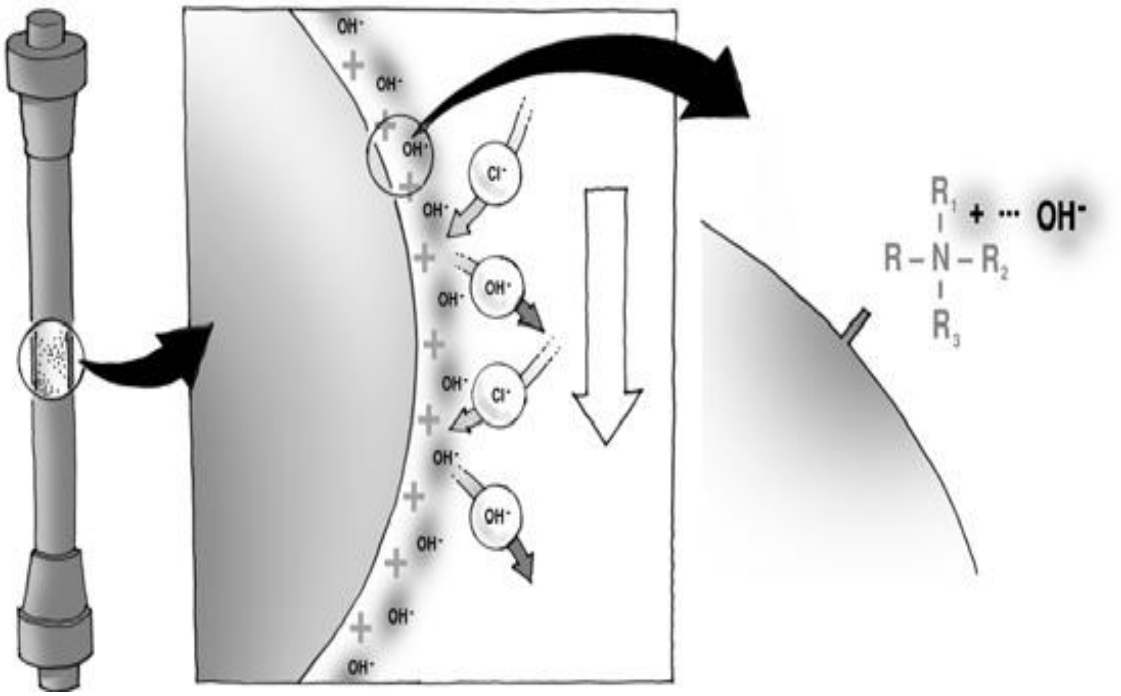

Figure 4.4: Mechanism of Ion Exchange in the Suppressor Column (A practical guide to ion chromatography, 2007). This figure demonstrates the ion exchange mechanism that occurs in the suppressor column. Sample ions bind to the charged groups of the stationary phase with different binding constants and are eluted in sequence by the eluent ion.

The main function of the analytical column is to separate the sample ions. Regardless of column type, they all contain charged packing material with ion exchange groups to aid in the separation process. In anion chromatography, the ion exchange groups are positively charged and made up of quaternary ammonium compounds (R-N+), with one of the groups being a carbon chain covalently bound to the resin. During the exchange reaction with the ion exchange groups, the sample ions separate as they move down the column due to their different binding constants.

4.3.7 Suppression

The eluent and sample ions go through a suppressor after leaving the column. By decreasing the eluent's conductivity, this apparatus improves sample ion detection. The suppressor slows the ions to varied degrees, depending on their properties, forcing them to reach the suppressor sequentially. Before reaching the detector, the suppressor transforms the eluent and analyte ions.

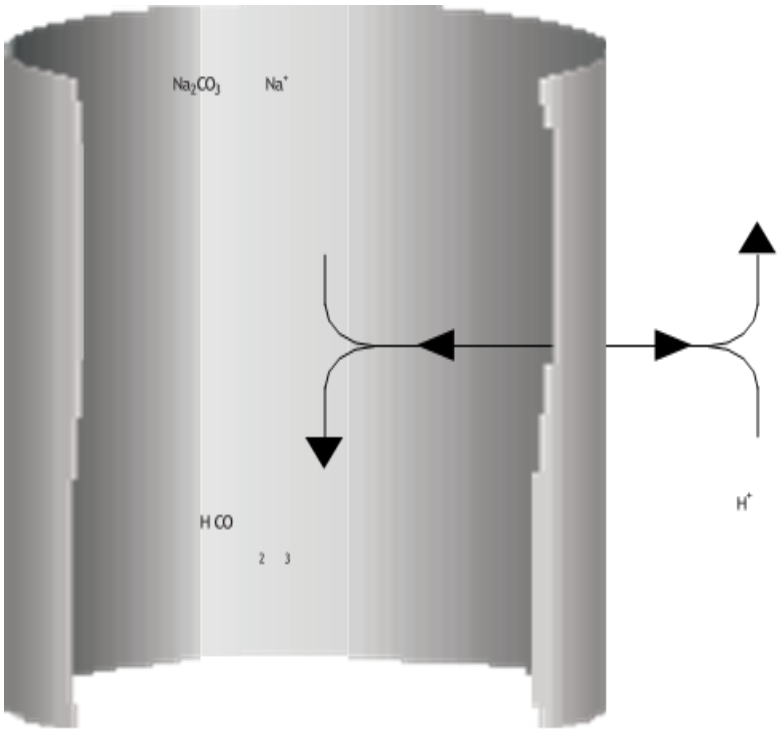

Figure 4.5: Schematic drawing of the ion exchange process in a membrane-based anion suppressor; (A practical guide to ion chromatography, 2007)

4.3.8 How Suppressor works

The eluent has a high conductivity since it contains a sizable amount of salt. To detect changes in eluate conductivity induced by ions at considerably lower concentrations than the eluent, the amount of dissolved ions in the eluent must be significantly reduced after the column. In other words, the suppressor's job is to reduce eluent conductivity. Suppression also increases the analyte ion signals. The eluent in the membrane suppressor is neutralized by continuous flow ion exchange across an ion exchange membrane, which reduces background conductivity. The eluent flows within a membrane tube, while the regenerant, a 5-50 mM acid, flows in the reverse direction outside the tube. When anions are separated with an alkaline eluent, a cation exchange occurs across the membrane: Na^+ or K^+ ions from the eluent are replaced by H^+ ions from the acid regenerant. Donnan exclusion, a form of electrostatic repulsion, prohibits anions in the eluate and the regenerant anion from passing through the membrane.

4.3.9 Detection

A conductivity cell measures the chemical conductance of sample ions as they exit the suppressor and generate a signal depending on a chemical or physical property of the analyte. The detector monitors the electrolytic conductivity of the eluate, and the suppressor serves two functions: it reduces the background of the eluent and increases sensitivity for sample ions. The detector signals can be analyzed manually using recorder charts or automatically using an integrator or a computer-based data-acquisition system with appropriate chromatographic software. The conductivity cell sends the signal to a data collection system, such as the Thermo Scientific™ Dionex™ Chromeleon™ 7 Chromatography Data System, which identifies the ions based on retention time and quantifies each analyte by integrating the peak area or height. The data is quantified by comparing sample peaks in a chromatogram to those produced by a standard solution. The results are shown as a chromatogram, and the amounts of ionic analytes are automatically computed and summarized.

4.4 Challenges and Solutions in using IC

Several challenges were faced when retrieving the data. The following is a summary of these difficulties and the solutions used to address them.

4.4.1 Short Retention Times

Causes:

- Rapid flow rate
- Use of improper eluents
- Column contamination

Resolution

- Prepared a new eluent, specifically the AS22 Eluent Concentrate (Sodium Carbonate/Bicarbonate Concentrate) from Thermo Fisher Scientific.
- Conducted a thorough column cleanup as follows:
    1. Prepared a 500 mL cleaning solution with 200 mM HCl in 80% acetonitrile.
    2. Disconnected the suppressor and directed the effluent to waste.
    3. Set the pump flow rate to 1.0 mL/min and separated the guard column from the analytical column.
    4. Rinsed both columns with deionized water for ten minutes.
    5. Cleaned each column individually with the acetonitrile-HCl solution for no less than sixty minutes.
    6. Rinsed the columns with deionized water for an additional ten minutes.
    7. Conditioned the columns with eluent for at least sixty minutes before resuming standard operations.

4.4.2 Inadequate Separation of Phosphate and Sulfate Peaks

Cause:

- Contamination of Sodium carbonate by Sodium hydroxide

Resolution:

- Prepared fresh eluents, sourced from Thermo Fisher Scientific, to ensure technical accuracy and purity.

4.4.3 Sample Carryover

Issue:

- Remnants of previous samples were detected in subsequent samples due to carryover in the autosampler rack.

Resolution:

- Extended the duration for which the sample probe remained in the rinse station.
- Thoroughly flushed the injection loop with at least 8 mL of deionized water before introducing the next sample, ensuring the elimination of residual traces

4.4.4 Excessive Pressure and Pressure Spikes During Injection

Issue:

- Excessive pressure and pressure spikes were observed during the injection process.

Resolution:

- Systematically replaced and maintained the seals of the pump head

4.5 Autosampler

4.5.1 Integration of Autosampler to IC

To automate the collection of individual anion peaks, an autosampler is integrated into the IC system. The autosampler model ASX 560 can efficiently gather 90 distinct samples within a 25-hour timeframe. A standard ASX 560 Autosampler comprises essential components such as the Z-Drive Assembly, Rinse Station, Arm, Standard Vials, Sample Vial Rack, and Sample Tray.

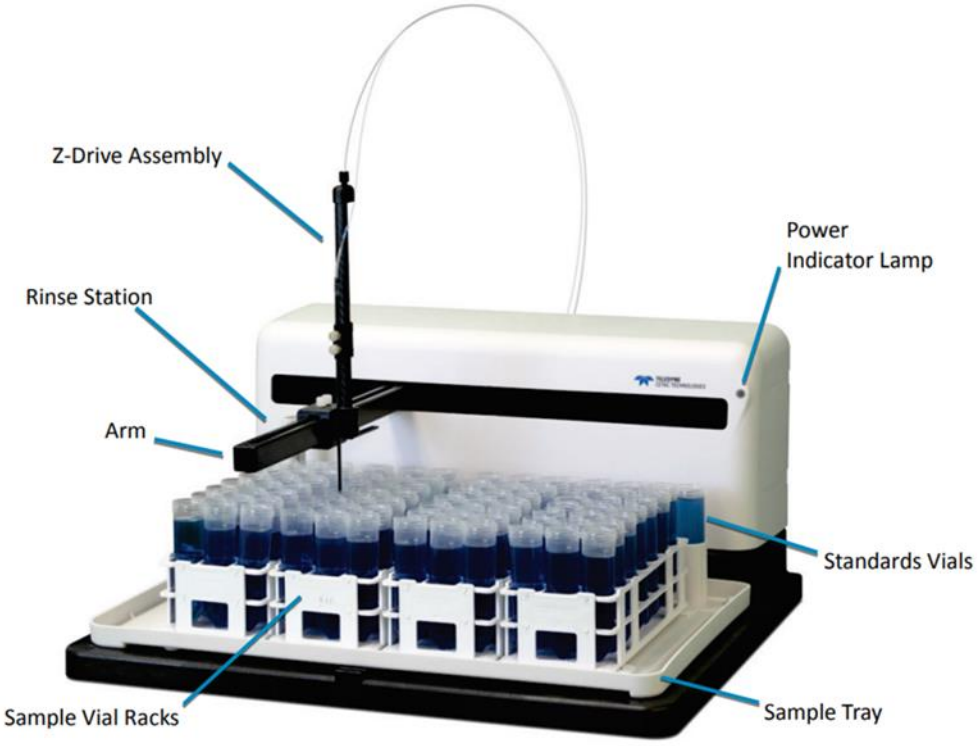

Figure 4.6: This figures shows the front view of the Autosampler and its components.The autosampler interfaces with the IC via connection cables. These cables include 1.823 meters of serial cables, linking the Z-Drive, Z-Drive motor, Sample Probe, and Injection Valve of the IC through the pump.

4.5.2 Automated sampling Process

The autosampler is programmed to initiate a sequence where, upon activation, the sample probe relocates to the rinse station and is lowered for rinsing. The pump is then activated and remains operational for approximately 120 seconds, aimed at cleansing the sample probe from any previously collected samples. After 120 seconds, the pump is deactivated, and the sample probe moves to the next tube. Subsequently, at the 5.5-minute mark, the pump is once again activated, running for about 210 seconds. This process facilitates the delivery of approximately 4 ml samples to the analytical column in the IC via the pump, as outlined earlier.

4.6 Results and Discussions

The objectives of the preparative mode are to accurately determine anion concentrations and to ensure efficient collection of fractions. Collection efficiency is achieved when a peak is completely separated from the ion chromatography system. A calibration curve was established using a series of standard solutions containing known concentrations of sulfate, nitrate, and chloride to calibrate both the concentration determination and peak retention times. In the analysis of anion concentrations, the preparative mode's efficacy in discerning anion concentrations was evaluated.

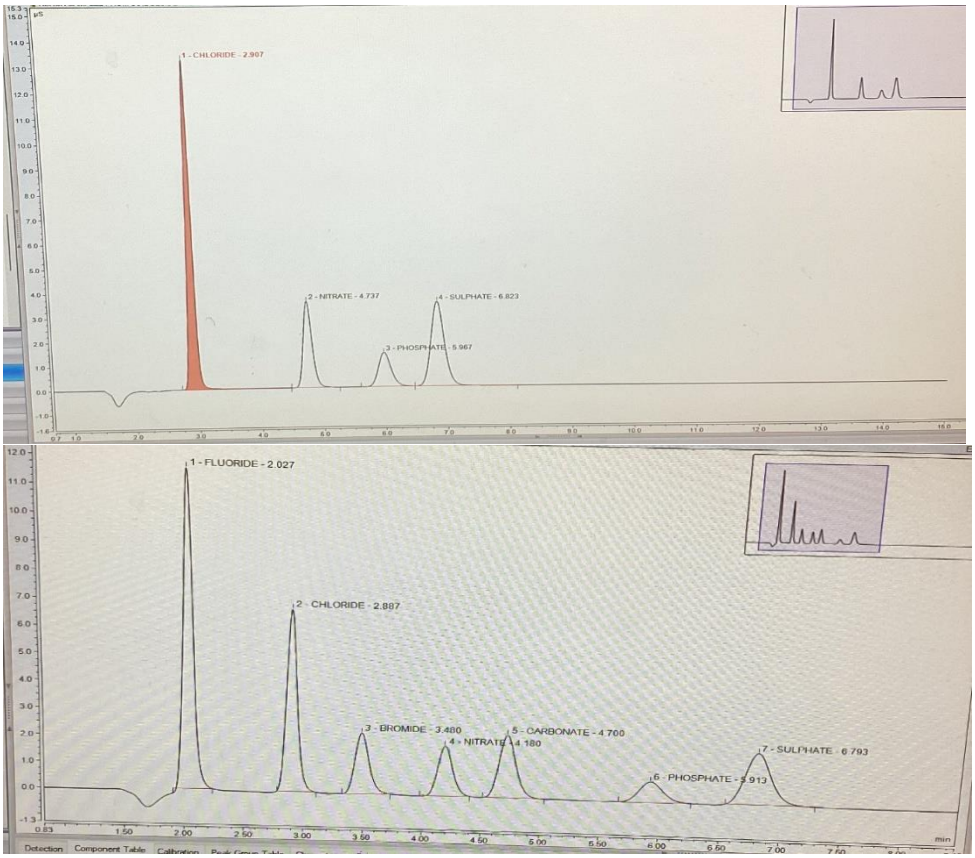

Figure 4.7: illustrates the chromatogram peaks. The chromatogram of the check standards is shown on the top panel, with the retention time peak indicated. The bottom panel displays the calibration standard's chromatogram, confirming the results' uniformity and reproducibility.

Standard solutions were prepared at concentrations of 1 ppm, 5 ppm, 10 ppm, and 100 ppm to ensure a wide calibration range (Fig 4.10). This approach ensured the conductivity peaks of anions were detectable at low concentrations and that the column capacity was not exceeded,

which would prevent effective separation at higher concentrations. The mixed standard solution was introduced onto the columns, and separation was achieved without peak overlap, even at off-scale peak heights. The successful detection of anions at low concentrations suggests that this preparative method is suitable for analyzing samples with low anion content.

Precision was determined by injecting an appropriate standard solution four or more times and evaluating peak heights or peak areas. This procedure evaluates the repeatability and consistency of measurements made in the same settings. Higher precision is indicated by lower relative standard deviations (RSDs), which display how close these measurements are when repeated under the same condition. For instance, the precision for 100, 50, 10, 5 and 1 ppm are ±0.33, ±1.05, ±0.80, ±0.17, ±0.60 respectively. Conversely, *accuracy* indicates the degree to which these measurements correspond with the true or accepted values. It represents the level of accuracy of the measurements. *Accuracy* is determined by examining numerous different standards and comparing the calibration curve results to known concentrations (actual value). The degree of consistency between these results and the true values aids in assessing the ion chromatography system's *accuracy*. A calibration curve is generated using a range of different standards, such as 1,5,10, 50, 100 ppm which is fitted with linear regression with a slope and R^2 as shown in fig 4.8.

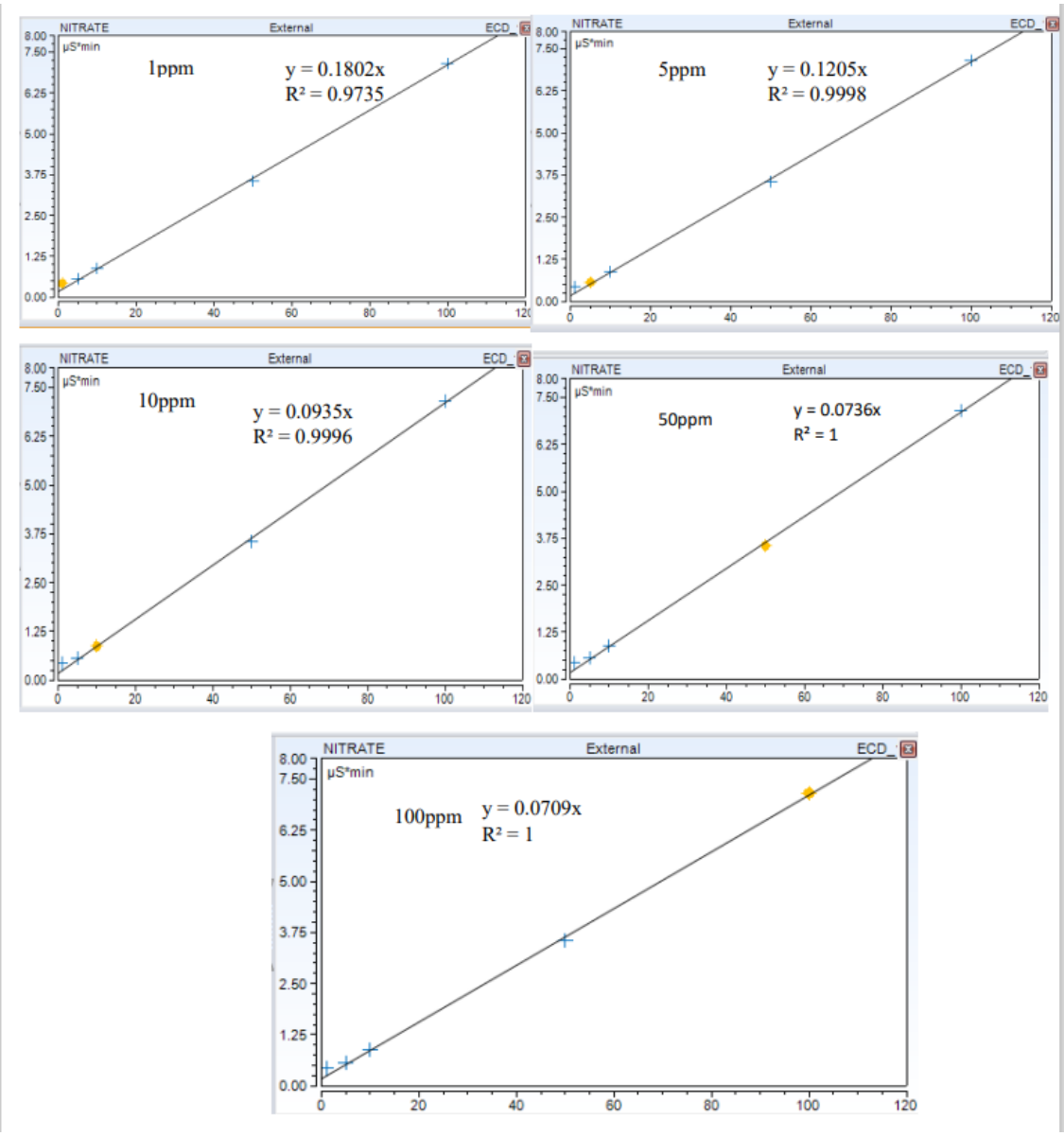

Figure 4.8: Calibration curve for different ppm levels of nitrate calibration standard solutions

A greater precision of the data is indicated by the calibration standards results, as all coefficients of determination (R^2) approach 1. Moreover, the calibration results demonstrate a strong correlation with the data, evidenced by an average standard deviation of 1.25 and an uncertainty of 0.47. The coefficient of determination measures how effectively the calibration model (linear regression) describes deviations from ion concentration data.

A high R^2 value (almost 1) indicates that the calibration curve correctly depicts the correlation between known concentrations and observed responses. A low R^2 value (near to zero) indicates that the calibration curve may not effectively represent this correlation.

5. CONCLUSION

In conclusion, this study's results cast doubt on the hypothesis that soil is the main source of nitrate in dust deposition in southern Nevada and California as portrayed by most USGS publications. While soil-derived dust makes some contribution to nitrate levels, the results show that other factors, such as atmospheric deposition and anthropogenic activities, also play important roles. The substantial variance in nitrate concentrations between traps and depths highlights the complexities of nitrate contents in this study site. Different sediments such as playas and alluvial plains have a substantial impact on nitrate distribution. Cima Volcanics (T30) has higher nitrate levels, due to previous lake deposits and scarce desert pavement, whereas Cadiz Lakes (T27) has lower levels, possibly due to vegetation and soil composition influencing nitrate uptake and leaching. The fraction of soil-derived nitrate ($f_{soil}NO_3^-$) is consistently low throughout all samples, never exceeding 0.03, implying that only a small proportion of the nitrate in the dust traps comes from the soil. The atmospheric nitrate percentage ($f_{atm}NO_3^-$), on the other hand, is typically close to or equal to 1. With atmospheric deposition and human activity playing a major role in increasing nitrate levels, the variations in nitrate concentrations between the soil and atmosphere further emphasize the influence of external factors and environmental factors.

Further, considering the minimal yearly precipitation in the study site, the study shows that wet deposition is not the main source of nitrate observed in the dust traps across most of the habitats tested. This is shown by the weak correlation found between nitrate deposition and Mean Annual Precipitation (MAP) and the wet nitrate deposition data from NADP, which suggests that rainfall has very little effect on nitrate levels.

Overall, the findings suggest that nitrate content at the study site is influenced by small quantities from both soil and wet atmospheric inputs. However, a significant portion may originate from nitric acid in dry atmospheric deposits, although this hypothesis is not supported by direct data or evidence in this thesis.

REFERENCES

A practical guide to ion chromatography (2007): An introduction and troubleshooting manual. SeQuent, Sweden.

Alfaro, L., Chanda, A., Kalemli-Ozcan, S., & Sayek, S. (2006). How Does Foreign Direct Investment Promote Economic Growth? Exploring the Effects of Financial Markets on Linkages (w12522; p. w12522). *National Bureau of Economic Research*. https://doi.org/10.3386/w12522

Al-Momani, I. F., Ya'qoub, A.-R. A., & Al-Bataineh, B. M. (2002). Atmospheric deposition of major ions and trace metals near an industrial area, Jordan. *Journal of Environmental Monitoring*, *4*(6), 985–989. https://doi.org/10.1039/b208697b

Álvarez, F., Reich, M., Snyder, G., Pérez-Fodich, A., Muramatsu, Y., Daniele, L., & Fehn, U. (2016). Iodine budget in surface waters from Atacama: Natural and anthropogenic iodine sources revealed by halogen geochemistry and iodine-129 isotopes. *Applied Geochemistry*, *68*, 53–63. https://doi.org/10.1016/j.apgeochem.2016.03.011

Amundson, R. (2004). Soil Formation. In *Treatise on Geochemistry, 5, Surface and Ground Water Weathering and Soils.* (p. P626). Elsevier.

Anderson, K., Wells, S., & Graham, R. (2002). Pedogenesis of Vesicular Horizons, Cima Volcanic Field, Mojave Desert, California. *Soil Science Society of America Journal*, *66*(3), 878–887. https://doi.org/10.2136/sssaj2002.8780

Barrie, L. A., & Sirois, A. (1986). *Wet And Dry Deposition Of Sulphates And Nitrates In Eastern Canada: 1979-1982*.

Blank, R. R., Young, J. A., & Allen, F. L. (1999). Aeolian dust in a saline playa environment, Nevada, U.S.A. *Journal of Arid Environments*, *41*(4), 365–381. https://doi.org/10.1006/jare.1998.0491

Bodenheimer, S., Lensky, I. M., & Dayan, U. (2019). Characterization of Eastern Mediterranean dust storms by area of origin; North Africa vs. Arabian Peninsula. *Atmospheric Environment*, *198*, 158–165. https://doi.org/10.1016/j.atmosenv.2018.10.034

Burns, D. A. (2003). Atmospheric nitrogen deposition in the Rocky Mountains of Colorado and southern Wyoming—A review and new analysis of past study results. *Atmospheric Environment*, *37*(7), 921–932. https://doi.org/10.1016/S1352-2310(02)00993-7

Butler, T., Likens, G., Vermeylen, F., & Stunder, B. (2005). The impact of changing nitrogen oxide emissions on wet and dry nitrogen deposition in the northeastern USA. *Atmospheric Environment*, *39*(27), 4851–4862. https://doi.org/10.1016/j.atmosenv.2005.04.031

Carlson, T. N., & Prospero, J. M. (1972). The Large-Scale Movement of Saharan Air Outbreaks over the Northern Equatorial Atlantic. *Journal of Applied Meteorology*, *11*(2), 283–297. https://doi.org/10.1175/1520-0450(1972)011<0283:TLSMOS>2.0.CO;2

Chadwick, O. A., Derry, L. A., Vitousek, P. M., Huebert, B. J., & Hedin, L. O. (1999). Changing sources of nutrients during four million years of ecosystem development. *Nature*, *397*(6719), 491–497. https://doi.org/10.1038/17276

Chester, Keyse, & Nimmo. (1996). *The Influence of Saharan and Middle Eastern Desert-Derived Dust on the Trace Metal Composition of Mediterranean Aerosols and Rainwaters: An Overview. In: Guerzoni S., Chester R. (eds) The Impact of Desert Dust Across the Mediterranean.: Vol. vol 11*. Environmental Science and Technology Library,. Springer, Dordrecht.

China, S., Burrows, S. M., Wang, B., Harder, T. H., Weis, J., Tanarhte, M., Rizzo, L. V., Brito, J., Cirino, G. G., Ma, P.-L., Cliff, J., Artaxo, P., Gilles, M. K., & Laskin, A. (2018). Fungal spores as a source of sodium salt particles in the Amazon basin. *Nature Communications*, *9*(1), 4793. https://doi.org/10.1038/s41467-018-07066-4

Clow, D. W., burns, G. P., Mast, M. A., Turk, J. T., & Campbell, D. H. (2002). Comparison of snowpack and winter wet-deposition chemistry in the Rocky Mountains, USA: Implications for winter dry deposition. *Atmospheric Environment*, *36*(14), 2337–2348. https://doi.org/10.1016/S1352-2310(02)00181-4

Crutzen, P. J. (1979). The Role of NO and NO_2^- in the Chemistry of the Troposphere and Stratosphere. *Annual Review of Earth and Planetary Sciences*, *7*(1), 443–472. https://doi.org/10.1146/annurev.ea.07.050179.002303

Daly, C., Neilson, R. P., & Phillips, D. L. (1994). A Statistical-Topographic Model for Mapping Climatological Precipitation over Mountainous Terrain. *Journal of Applied Meteorology*, *33*(2), 140–158. https://doi.org/10.1175/1520-0450(1994)033<0140:ASTMFM>2.0.CO;2

Daly, C., Taylor, G., & Gibson, W. (1997). *The Prism Approach to Mapping Precipitation and Temperature*.

Dan, J., Yaalon, D. H., & Koyumdjisky, H. (1969). Catenary soil relationships in Israel, 1. The netanya cate na on coastal dunes of the sharon. *Geoderma*, *2*(2), 95–120. https://doi.org/10.1016/0016-7061(69)90018-4

Dionex Aquion Ion Chromatography System Operator's Manual. (2016). Thermo Fisher Scientific Inc.

D'Odorico, P., Caylor, K., Okin, G. S., & Scanlon, T. M. (2007). On soil moisture–vegetation feedbacks and their possible effects on the dynamics of dryland ecosystems. *Journal of Geophysical Research: Biogeosciences*, *112*(G4), 2006JG000379. https://doi.org/10.1029/2006JG000379

Driscoll, C. T., & Martins, I. (2019). Ecological Effects of Acidic Deposition. In *Encyclopedia of Ecology* (pp. 315–324). Elsevier. https://doi.org/10.1016/B978-0-12-409548-9.00847-2

Du, E., De Vries, W., Galloway, J. N., Hu, X., & Fang, J. (2014). Changes in wet nitrogen deposition in the United States between 1985 and 2012. *Environmental Research Letters*, *9*(9), 095004. https://doi.org/10.1088/1748-9326/9/9/095004

Ducloux, J., Petit, S., Decarreau, A., & Delhoume, J. P. (1995). Clay Differentiation in Aridisols of Northern Mexico. *Soil Science Society of America Journal*, *59*(1), 269–276. https://doi.org/10.2136/sssaj1995.03615995005900010043x

Duniway, M. C., Pfennigwerth, A. A., Fick, S. E., Nauman, T. W., Belnap, J., & Barger, N. N. (2019). Wind erosion and dust from US drylands: A review of causes, consequences, and solutions in a changing world. *Ecosphere*, *10*(3), e02650. https://doi.org/10.1002/ecs2.2650

Dwyer, D. D., Hastings, J. R., & Turner, R. M. (1966). The Changing Mile: An Ecological Study of Vegetation Change with Time in the Lower Mile of An Arid and Semiarid Region. *Journal of Range Management*, *19*(3), 156. https://doi.org/10.2307/3895408

Elliott, E. M., Kendall, C., Wankel, S. D., Burns, D. A., Boyer, E. W., Harlin, K., Bain, D. J., & Butler, T. J. (2007). Nitrogen Isotopes as Indicators of NO_x Source Contributions to Atmospheric Nitrate Deposition Across the Midwestern and Northeastern United States. *Environmental Science & Technology*, *41*(22), 7661–7667. https://doi.org/10.1021/es070898t

Engelstaedter, S., Tegen, I., & Washington, R. (2006). North African dust emissions and transport. *Earth-Science Reviews*, *79*(1–2), 73–100. https://doi.org/10.1016/j.earscirev.2006.06.004

Finlayson-Pitts, B. J., & Pitts, J. N. (2000). Acid Deposition. In *Chemistry of the Upper and Lower Atmosphere* (pp. 294–348). Elsevier. https://doi.org/10.1016/B978-012257060-5/50010-1

Floyd, K. W., & Gill, T. E. (2011). The association of land cover with aeolian sediment production at Jornada Basin, New Mexico, USA. *Aeolian Research*, *3*(1), 55–66. https://doi.org/10.1016/j.aeolia.2011.02.002

Galloway, J. N., Dentener, F. J., Capone, D. G., Boyer, E. W., Howarth, R. W., Seitzinger, S. P., Asner, G. P., Cleveland, C. C., Green, P. A., Holland, E. A., Karl, D. M., Michaels, A. F., Porter, J. H., Townsend, A. R., & Vosmarty, C. J. (2004). Nitrogen Cycles: Past, Present, and Future. *Biogeochemistry*, *70*(2), 153–226. https://doi.org/10.1007/s10533-004-0370-0

Galloway, J. N., Thornton, J. D., Norton, S. A., Volchok, H. L., & McLean, R. A. N. (1982). Trace metals in atmospheric deposition: A review and assessment. *Atmospheric Environment (1967)*, *16*(7), 1677–1700. https://doi.org/10.1016/0004-6981(82)90262-1

Gibson, E. K., Wentworth, S. J., & McKay, D. S. (1983). Chemical weathering and diagenesis of a cold desert soil from Wright Valley, Antarctica: An analog of Martian weathering processes. *Journal of Geophysical Research: Solid Earth*, *88*(S02). https://doi.org/10.1029/JB088iS02p0A912

Gill, T. E. (1996). Eolian sediments generated by anthropogenic disturbance of playas: Human impacts on the geomorphic system and geomorphic impacts on the human system. *Geomorphology*, *17*(1–3), 207–228. https://doi.org/10.1016/0169-555X(95)00104-D

Glaser, P. H., Hansen, B. C. S., Donovan, J. J., Givnish, T. J., Stricker, C. A., & Volin, J. C. (2013). Holocene dynamics of the Florida Everglades with respect to climate, dustfall, and tropical storms. *Proceedings of the National Academy of Sciences*, *110*(43), 17211–17216. https://doi.org/10.1073/pnas.1222239110

Graham, R. C., Hirmas, D. R., Wood, Y. A., & Amrhein, C. (2008). Large near-surface nitrate pools in soils capped by desert pavement in the Mojave Desert, California. *Geology*, *36*(3), 259. https://doi.org/10.1130/G24343A.1

Greeley, & Iversen. (1985). *Wind as a Geological Process on Earth, Mars, Venus, and Titan*. (New York: Cambridge University Press).

Gruber, N., & Galloway, J. N. (2008). An Earth-system perspective of the global nitrogen cycle. *Nature*, *451*(7176), 293–296. https://doi.org/10.1038/nature06592

Gu, C., & Riley, W. J. (2010). Combined effects of short-term rainfall patterns and soil texture on soil nitrogen cycling—A modeling analysis. *Journal of Contaminant Hydrology*, *112*(1–4), 141–154. https://doi.org/10.1016/j.jconhyd.2009.12.003

Guerzoni, S., Molinaroli, E., & Chester, R. (1997). Saharan dust inputs to the western Mediterranean Sea: Depositional patterns, geochemistry and sedimentological implications. *Deep Sea Research Part II: Topical Studies in Oceanography*, *44*(3–4), 631–654. https://doi.org/10.1016/S0967-0645(96)00096-3

Guieu, C., Loÿe-Pilot, M. -D., Ridame, C., & Thomas, C. (2002). Chemical characterization of the Saharan dust end-member: Some biogeochemical implications for the western Mediterranean Sea. *Journal of Geophysical Research: Atmospheres*, *107*(D15). https://doi.org/10.1029/2001JD000582

Hall, T. C., & Blacet, F. E. (1952). Separation of the Absorption Spectra of NO_2^- and N_2O_4 in the Range of 2400–5000A. *The Journal of Chemical Physics*, *20*(11), 1745–1749. https://doi.org/10.1063/1.1700281

Halstead, M. J. R., Cunninghame, R. G., & Hunter, K. A. (2000). Wet deposition of trace metals to a remote site in Fiordland, New Zealand. *Atmospheric Environment*, *34*(4), 665–676. https://doi.org/10.1016/S1352-2310(99)00185-5

Hov, Øystein. (1987). *The Abatement Of Photochemical Oxidants In Europe. Calculations In The Support Of Oecd's Project "Control Of Major Air Pollutants.* Nilu.

Huang, K., Zhuang, G., Li, J., Wang, Q., Sun, Y., Lin, Y., & Fu, J. S. (2010). Mixing of Asian dust with pollution aerosol and the transformation of aerosol components during the dust storm over China in spring 2007. *Journal of Geophysical Research: Atmospheres*, *115*(D7), 2009JD013145. https://doi.org/10.1029/2009JD013145

Hunter, R. B., Romney, E. M., & Wallace, A. (1982). Nitrate Distribution In Mojave Desert Soils: *Soil Science*, *134*(1), 22–30. https://doi.org/10.1097/00010694-198207000-00004

Keresztesi, Á., Nita, I.-A., Boga, R., Birsan, M.-V., Bodor, Z., & Szép, R. (2020). Spatial and long-term analysis of rainwater chemistry over the conterminous United States. *Environmental Research*, *188*, 109872. https://doi.org/10.1016/j.envres.2020.109872

Langbein, W. (1961). *Salinity and Hydrology of Closed Lakes* (Professional Paper) [Professional Paper].

Leah, T., Cerbari, V., Baliuk, S., Zakharova, M., & Nosonenko, O. (2018). *Physical Properties Features Of Alluvial Irrigated Soils Of Dniester And Dnieper River Basins*.

Logan, J. A. (1983). Nitrogen oxides in the troposphere: Global and regional budgets. *Journal of Geophysical Research: Oceans*, *88*(C15), 10785–10807. https://doi.org/10.1029/JC088iC15p10785

MacMahon J.A, & Wagner F.H.,. (1985). *In Hot Deserts and Arid Shrublands, A; The Mojave, Sonoran, and Chihuahuan deserts of North America; Evenari, M.; Noy-Meir, I.; Goodall, D.W.; Ecosystems of the World, Amsterdam,: Vol. 12A,*.

Marion, G. M., Verburg, P. S. J., Stevenson, B., & Arnone, J. A. (2008). Soluble Element Distributions in a Mojave Desert Soil. *Soil Science Society of America Journal*, *72*(6), 1815–1823. https://doi.org/10.2136/sssaj2007.0240

Marrett, D. J., Khattak, R. A., Elseewi, A. A., & Page, A. L. (1990). Elevated Nitrate Levels in Soils of the Eastern Mojave Desert. *Journal of Environmental Quality*, *19*(4), 658–663. https://doi.org/10.2134/jeq1990.00472425001900040005x

Martens-Habbena, W., Berube, P. M., Urakawa, H., De La Torre, J. R., & Stahl, D. A. (2009). Ammonia oxidation kinetics determine niche separation of nitrifying Archaea and Bacteria. *Nature*, *461*(7266), 976–979. https://doi.org/10.1038/nature08465

McAuliffe, J. R. (1994). Landscape Evolution, Soil Formation, and Ecological Patterns and Processes in Sonoran Desert Bajadas. *Ecological Monographs*, *64*(2), 111–148. https://doi.org/10.2307/2937038

McFadden, L. D., Wells, S. G., & Jercinovich, M. J. (1987). Influences of eolian and pedogenic processes on the origin and evolution of desert pavements. *Geology*, *15*(6), 504. https://doi.org/10.1130/0091-7613(1987)15<504:IOEAPP>2.0.CO;2

Michael Rosen. (1994). *Paleoclimate and Basin Evolution of Playa Systems* (Vol. 289). Geological Society of America. https://doi.org/10.1130/SPE289

Muhs, D. R., Budahn, J. R., Prospero, J. M., Skipp, G., & Herwitz, S. R. (2012). Soil genesis on the island of Bermuda in the Quaternary: The importance of African dust transport and deposition. *Journal of Geophysical Research: Earth Surface*, *117*(F3), 2012JF002366. https://doi.org/10.1029/2012JF002366

Nettleton, W. D., Witty, J. E., Nelson, R. E., & Hawley, J. W. (1975). Genesis of Argillic Horizons in Soils of Desert Areas of the Southwestern United States. *Soil Science Society of America Journal*, *39*(5), 919–926. https://doi.org/10.2136/sssaj1975.03615995003900050035x

Nick Middleton & Andrew Goudie. (2006). *Desert Dust in the Global System*. Springer Berlin Heidelberg. https://doi.org/10.1007/3-540-32355-4

Nriagu, J. O., & Pacyna, J. M. (1988). Quantitative assessment of worldwide contamination of air, water and soils by trace metals. *Nature*, *333*(6169), 134–139. https://doi.org/10.1038/333134a0

Peretti, M., Piñeiro, G., Fernández Long, M. E., & Carnelos, D. A. (2020). Influence of the precipitation interval on wet atmospheric deposition. *Atmospheric Environment*, *237*, 117580. https://doi.org/10.1016/j.atmosenv.2020.117580

Pérez-Fodich, A., Reich, M., Álvarez, F., Snyder, G. T., Schoenberg, R., Vargas, G., Muramatsu, Y., & Fehn, U. (2014). Climate change and tectonic uplift triggered the formation of the Atacama Desert's giant nitrate deposits. *Geology*, *42*(3), 251–254. https://doi.org/10.1130/G34969.1

Prospero, J. M., & Carlson, T. N. (1972). Vertical and areal distribution of Saharan dust over the western equatorial north Atlantic Ocean. *Journal of Geophysical Research*, *77*(27), 5255–5265. https://doi.org/10.1029/JC077i027p05255

Prospero, J. M., Ginoux, P., Torres, O., Nicholson, S. E., & Gill, T. E. (2002). Environmental Characterization Of Global Sources Of Atmospheric Soil Dust Identified With The Nimbus 7 Total Ozone Mapping Spectrometer (Toms) Absorbing Aerosol Product. *Reviews of Geophysics*, *40*(1). https://doi.org/10.1029/2000RG000095

Pye, K. (1987). *Aeolian Dust and Dust Deposits*. (London: Academic).

Querol, X., Tobías, A., Pérez, N., Karanasiou, A., Amato, F., Stafoggia, M., Pérez García-Pando, C., Ginoux, P., Forastiere, F., Gumy, S., Mudu, P., & Alastuey, A. (2019). Monitoring the impact of desert dust outbreaks for air quality for health studies. *Environment International*, *130*, 104867. https://doi.org/10.1016/j.envint.2019.05.061

Reheis. (2003). *Dust Deposition in Nevada, California, and Utah,1984-2002*.

Reheis, M. C. (1990). Influence of climate and eolian dust on the major-element chemistry and clay mineralogy of soils in the northern Bighorn basin, U.S.A. *CATENA*, *17*(3), 219–248. https://doi.org/10.1016/0341-8162(90)90018-9

Reheis, M. C. (1997). Dust deposition downwind of Owens (dry) Lake, 1991–1994: Preliminary findings. *Journal of Geophysical Research: Atmospheres*, *102*(D22), 25999–26008. https://doi.org/10.1029/97JD01967

Reheis, M. C., Budahn, J. R., & Lamothe, P. J. (2002). Geochemical evidence for diversity of dust sources in the southwestern United States. *Geochimica et Cosmochimica Acta*, *66*(9), 1569–1587. https://doi.org/10.1016/S0016-7037(01)00864-X

Reheis, M. C., Budahn, J. R., Lamothe, P. J., & Reynolds, R. L. (2009). Compositions of modern dust and surface sediments in the Desert Southwest, United States. *Journal of Geophysical Research: Earth Surface*, *114*(F1), 2008JF001009. https://doi.org/10.1029/2008JF001009

Reheis, M. C., Goodmacher, J. C., Harden, J. W., McFadden, L. D., Rockwell, T. K., Shroba, R. R., Sowers, J. M., & Taylor, E. M. (1995). Quaternary soils and dust deposition in southern Nevada and California. *Geological Society of America Bulletin*, *107*(9), 1003–1022. https://doi.org/10.1130/0016-7606(1995)107<1003:QSADDI>2.3.CO;2

Reheis, M. C., & Kihl, R. (1995). Dust deposition in southern Nevada and California, 1984–1989: Relations to climate, source area, and source lithology. *Journal of Geophysical Research: Atmospheres*, *100*(D5), 8893–8918. https://doi.org/10.1029/94JD03245

Reheis, M. C., Sowers, J. M., Taylor, E. M., McFadden, L. D., & Harden, J. W. (1992). Morphology and genesis of carbonate soils on the Kyle Canyon fan, Nevada, U.S.A. *Geoderma*, *52*(3–4), 303–342. https://doi.org/10.1016/0016-7061(92)90044-8

Reynolds, R. L., Bogle, R., Vogel, J., Goldstein, H., & Yount, J. (2009). *Dust Emission at Franklin Lake Playa, Mojave Desert (USA): Response to Meteorological and Hydrologic Changes 2005–2008*. *15*.

Reynolds, R., Yount, J., Reheis, M., Goldstein, H., Forester, R., & Fulton, R. (2006). *Dust emission from playas in the Mojave Desert, USA*.

Rosenstock, N. P., Stendahl, J., Van Der Heijden, G., Lundin, L., McGivney, E., Bishop, K., & Löfgren, S. (2019). Base cations in the soil bank: Non-exchangeable pools may sustain centuries of net loss to forestry and leaching. *SOIL*, *5*(2), 351–366. https://doi.org/10.5194/soil-5-351-2019

Shao, Y., Raupach, M. R., & Findlater, P. A. (1993). Effect of saltation bombardment on the entrainment of dust by wind. *Journal of Geophysical Research: Atmospheres*, *98*(D7), 12719–12726. https://doi.org/10.1029/93JD00396

Shaw, P.A. & Thomas, D.S.G. (1989). *Playas, pans, and salt lakes. In: Thomas, D.S.G. (ed), Arid Zone Ggeomorphology*. Belhaven Press, London:

Sickles, J. E., & Shadwick, D. S. (2007). Seasonal and regional air quality and atmospheric deposition in the eastern United States. *Journal of Geophysical Research: Atmospheres*, *112*(D17), 2006JD008356. https://doi.org/10.1029/2006JD008356

Stevenson, F. J. (Ed.). (1982). *Nitrogen in Agricultural Soils*. American Society of Agronomy, Crop Science Society of America, Soil Science Society of America. https://doi.org/10.2134/agronmonogr22

Tanaka, K. (2000). Dust and Ice Deposition in the Martian Geologic Record. *Icarus*, *144*(2), 254–266. https://doi.org/10.1006/icar.1999.6297

Tao, S., Fang, J., Zhao, X., Zhao, S., Shen, H., Hu, H., Tang, Z., Wang, Z., & Guo, Q. (2015). Rapid loss of lakes on the Mongolian Plateau. *Proceedings of the National Academy of Sciences*, *112*(7), 2281–2286. https://doi.org/10.1073/pnas.1411748112

Taylor, G., & Daly, C. (2004). *Using PRISM Climate Grids and GIS for Extreme Precipitation Mapping*. Oregon State University.

Tegen, I., & Fung, I. (1994). Modeling of mineral dust in the atmosphere: Sources, transport, and optical thickness. *Journal of Geophysical Research: Atmospheres*, *99*(D11), 22897–22914. https://doi.org/10.1029/94JD01928

Tuncer, B., Bayar, B., Yeşilyurt, C., & Tuncel, G. (2001). Ionic composition of precipitation at the Central Anatolia (Turkey). *Atmospheric Environment*, *35*(34), 5989–6002. https://doi.org/10.1016/S1352-2310(01)00396-X

USGS. (2000). *Atmospheric Deposition Program of the U.S. Geological Survey*.

Vitousek, P. M., Kennedy, M. J., Derry, L. A., & Chadwick, O. A. (1999). Weathering versus atmospheric sources of strontium in ecosystems on young volcanic soils. *Oecologia*, *121*(2), 255–259. https://doi.org/10.1007/s004420050927

Voigt, C., Klipsch, S., Herwartz, D., Chong, G., & Staubwasser, M. (2020). The spatial distribution of soluble salts in the surface soil of the Atacama Desert and their relationship to hyperaridity. *Global and Planetary Change*, *184*, 103077. https://doi.org/10.1016/j.gloplacha.2019.103077

Walvoord, M. A., Phillips, F. M., Stonestrom, D. A., Evans, R. D., Hartsough, P. C., Newman, B. D., & Striegl, R. G. (2003). A Reservoir of Nitrate Beneath Desert Soils. *Science*, *302*(5647), 1021–1024. https://doi.org/10.1126/science.1086435

Washington, R., Todd, M. C., Lizcano, G., Tegen, I., Flamant, C., Koren, I., Ginoux, P., Engelstaedter, S., Bristow, C. S., Zender, C. S., Goudie, A. S., Warren, A., & Prospero, J. M. (2006). Links between topography, wind, deflation, lakes and dust: The case of the Bodélé Depression, Chad. *Geophysical Research Letters*, *33*(9), 2006GL025827. https://doi.org/10.1029/2006GL025827

Wood, Y. A., Graham, R. C., & Wells, S. G. (2002). Surface mosaic map unit development for a desert pavement surface. *Journal of Arid Environments*, *52*(3), 305–317. https://doi.org/10.1006/jare.2002.1006

Wu, F., Cheng, Y., Hu, T., Song, N., Zhang, F., Shi, Z., Hang Ho, S. S., Cao, J., & Zhang, D. (2022). Saltation–Sandblasting Processes Driving Enrichment of Water-Soluble Salts in Mineral Dust. *Environmental Science & Technology Letters*, *9*(11), 921–928. https://doi.org/10.1021/acs.estlett.2c00652

Xu-Yang, Y., Dessert, C., & Losno, R. (2022). Atmospheric Deposition Over the Caribbean Region: Sea Salt and Saharan Dust Are Sources of Essential Elements on the Island of Guadeloupe. *Journal of Geophysical Research: Atmospheres*, *127*(22), e2022JD037175. https://doi.org/10.1029/2022JD037175

Young, J. A., & Evans, R. A. (1986). Erosion and deposition of fine sediments from playas. *Journal of Arid Environments*, *10*(2), 103–115. https://doi.org/10.1016/S0140-1963(18)31251-5

Yu, H., Chin, M., Yuan, T., Bian, H., Remer, L. A., Prospero, J. M., Omar, A., Winker, D., Yang, Y., Zhang, Y., Zhang, Z., & Zhao, C. (2015). The fertilizing role of African dust in the Amazon rainforest: A first multiyear assessment based on data from Cloud-Aerosol Lidar and Infrared Pathfinder Satellite Observations. *Geophysical Research Letters*, *42*(6), 1984–1991. https://doi.org/10.1002/2015GL063040

Zhang, Q., Li, Y., Wang, M., Wang, K., Meng, F., Liu, L., Zhao, Y., Ma, L., Zhu, Q., Xu, W., & Zhang, F. (2021). Atmospheric nitrogen deposition: A review of quantification methods and its spatial pattern derived from the global monitoring networks. *Ecotoxicology and Environmental Safety*, *216*, 112180. https://doi.org/10.1016/j.ecoenv.2021.112180

Zhang, X., Zhao, L., Cheng, M., Liu, H., Wang, Z., Wu, X., & Yu, H. (2018). Long-term changes in wet nitrogen and sulfur deposition in Nanjing. *Atmospheric Environment*, *195*, 104–111. https://doi.org/10.1016/j.atmosenv.2018.09.048

Zhao, S., Yu, Y., He, J., Yin, D., & Wang, B. (2015). Below-cloud scavenging of aerosol particles by precipitation in a typical valley city, northwestern China. *Atmospheric Environment*, *102*, 70–78. https://doi.org/10.1016/j.atmosenv.2014.11.051

Zhao, S., Yu, Y., Yin, D., Liu, N., & He, J. (2014). Ambient particulate pollution during Chinese Spring Festival in urban Lanzhou, Northwestern China. *Atmospheric Pollution Research*, *5*(2), 335–343. https://doi.org/10.5094/APR.2014.039

Zucca, C., Middleton, N., Kang, U., & Liniger, H. (2021). Shrinking water bodies as hotspots of sand and dust storms: The role of land degradation and sustainable soil and water management. *CATENA*, *207*, 105669. https://doi.org/10.1016/j.catena.2021.105669